Photocatalytic degradation of 2-chlorophenol by synthesizing novel and visible light active Aluminum doped ZnTiO₃

وَمَن يُؤْتَ الحِكمَةَ
فَقَد أوتِيَ خَيرًا كثيرًا

QUAID-I-AZAM UNIVERSITY

ISLAMABAD

MASTER OF PHILOSOPHY

In

Environmental Sciences

By

Iqra Perveen
Registration No. 02311911010
Supervised by: Dr. Jamshaid Rashid

Department of Environmental Sciences
Faculty of Biological Sciences
Quaid-i-Azam University, Islamabad
2019-2022

Photocatalytic degradation of 2-chlorophenol by synthesizing novel and visible light active Aluminum doped ZnTiO₃

وَمَن يُؤتَ الحِكمَةَ
فَقَد أوتِيَ خَيرًا كَثيرًا

QUAID-I-AZAM UNIVERSITY

ISLAMABAD

A Thesis Submitted in Partial Fulfillment of the Requirement for the Degree

MASTER OF PHILOSOPHY
In
Environmental Sciences

By

Iqra Perveen
Registration No. 02311911010
Supervised by: Dr. Jamshaid Rashid

Department of Environmental Sciences
Faculty of Biological Sciences
Quaid-i-Azam University, Islamabad
2019-2022

To my Ammi and Abbu

for their Faith, Endless love, Support, &

Encouragement.

CERTIFICATE OF APPROVAL

It is to certify that the research work presented in this thesis, entitled **"Photocatalytic degradation of 2-Chlorophenol by synthesizing a novel and visible light active Aluminum doped ZnTiO₃"** was conducted by **Ms. Iqra Perveen** (Reg. 02311911010) under the supervision of **Dr. Jamshaid Rashid**. No part of this thesis has been submitted else for any other degree. This thesis is submitted to the Department of Environmental Sciences, in the partial fulfilment of the requirements for the degree of **Master of Philosophy (M.Phil.)** in the field of Environmental Sciences, Quaid-i-Azam University, Islamabad.

Iqra Perveen (M.Phil. Scholar)

Supervisor:

Dr. Jamshaid Rashid   _____

Associate Professor

Department of Environmental Sciences

Quaid-i-Azam University, Islamabad, Pakistan

External Examiner:

Dr. Qaiser Hussain   _____

Associate Professor

Institute of Soil Sciences

Pir Mehr Ali Shah Arid Agriculture University, Rawalpindi

Chairman:

Dr. Sohail Yousaf   _____

Department of Environmental Sciences

Quaid-i-Azam University, Islamabad

Dated: 27-1-2022

AUTHOR'S DECLARATION

I, **"Iqra Perveen"** (Registration No. 0211911010) hereby declare that my M.Phil. thesis titled as **"Photocatalytic Degradation of 2-Chlorophenol by Synthesizing a Novel and Visible Light Aluminum doped ZnTiO₃"** is all my own effort done in Renewable Energy Advancement Laboratory, Department of Environmental Sciences, Quaid-i-Azam University, Islamabad. All the investigations, findings, results, conclusion of this research has neither been previously presented anywhere nor published in any local or international forum.

Iqra Perveen

PLAGIARISM UNDERTAKING

I, **Iqra Perveen**, hereby state that my M.Phil. thesis titled as **"Photocatalytic Degradation of 2-Chlorophenol by Synthesizing a Novel and Visible Light Active Aluminum Doped ZnTiO₃"** is solely my research work with no significant contribution from any other person. Small contribution/help whatever taken has been duly acknowledged and that complete thesis has been written by me.

I understand zero tolerance policy of the HEC and Quaid-i-Azam University, Islamabad, towards plagiarism. Therefore, I as an author of the above titled thesis declare that no portion of my thesis has been plagiarized and any material used as reference is properly referred/cited.

I undertake that if I am found guilty of any form of plagiarism in the above titled thesis even after the award of M.Phil. degree, the university reserves the right to withdraw/revoke my M.Phil. degree and that HEC and the university has the right to publish my name on the HEC/University website on which the names of students are placed who submitted plagiarism.

Iqra Perveen

Table of Contents

ACKNOWLEDGMENT

LIST OF ABBREVIATIONS

°C	Degree Celsius
2-CP	2-Chlorophenol
Al-ZnTiO$_3$	Aluminum doped Zinc Titanate
AOPs	Advanced Oxidation Processes
CB	Conduction Band
CO$_2$	Carbon Dioxide
eV	Electron Volt
g	Gram
h	Hours
mg	Milligram
Min	Minutes
Nm	Nanometer
O$_2$	Oxygen
pH	Negative log of Hydrogen
PL	Photoluminescence
TiO$_2$	Titania
TNT	Titania Nanotubes
UV-Vis DRS	Ultraviolet-Visible Diffused Reflctance Spectroscopy
VB	Valance Band
XRD	X-Ray Diffraction
ZnO	Zinc Oxide
ZnTiO$_3$	Zinc Titanate

LIST OF FIGURES

LIST OF TABLES

ABSTRACT

This study focuses on the elimination of priority organic pollutants from wastewater because of their severe effects on the environment. Conventional treatment methods are inefficient to treat organic pollutants; instead, they result in the production of more toxic compounds that are hazardous for ecosystem as well as human beings. Therefore, a semiconductor $ZnTiO_3$ with Aluminum doping is designed with simple synthesis steps and its activity was observed under direct sunlight for efficient catalytic oxidation of Phenolic compound known as 2-Chlorophenol. The physiochemical properties of all the prepared catalysts were investigated via XRD, UV-Vis DRS and PL. 1% Al-$ZnTiO_3$ showed maximum photocatalytic degradation among all photocatalysts prepared. The calculated band gap of all nano catalysts i.e., TNT, $ZnTiO_3$, 3% Al-$ZnTiO_3$, 1% Al-$ZnTiO_3$ are 3.22 eV, 3.04 eV, 2.93 eV, and 2.81 eV respectively. Experiments were performed to study the key parameters of photo-catalysis that includes the effect of pH, initial concentration of the 2-CP, catalyst dosage and reusability of the catalyst. 1% Al-$ZnTiO_3$ showed maximum photocatalytic degradation activity at pH 6 that was normal pollutant solution pH. Initial concentration of 20 mgL^{-1} 2-chlorophenol was found to be the most efficient for photocatalytic degradation that exhibited about 98.96% degradation, using 0.5 gL^{-1} within 180 minutes at pH 6. Optimum results were obtained for all catalysts at 100 mgL-1 2-Chlorophenol concentration, 0.5 gL-1 catalyst dose, and pH 6. Furthermore, reusability tests demonstrated the remarkable stability of 1% Al-$ZnTiO_3$ photocatalyst, which maintained high activity even after several cycles of reuse. The results obtained during the study demonstrate the potential of photocatalytic degradation of 2-CP under direct solar light, indicating that the synthesized 1% Al-ZnTiO3 photocatalyst is effective for efficient catalytic oxidation of the phenolic compound. These findings provide evidence for the feasibility of using photocatalytic methods to eliminate priority organic pollutants from wastewater.

Graphical Abstract
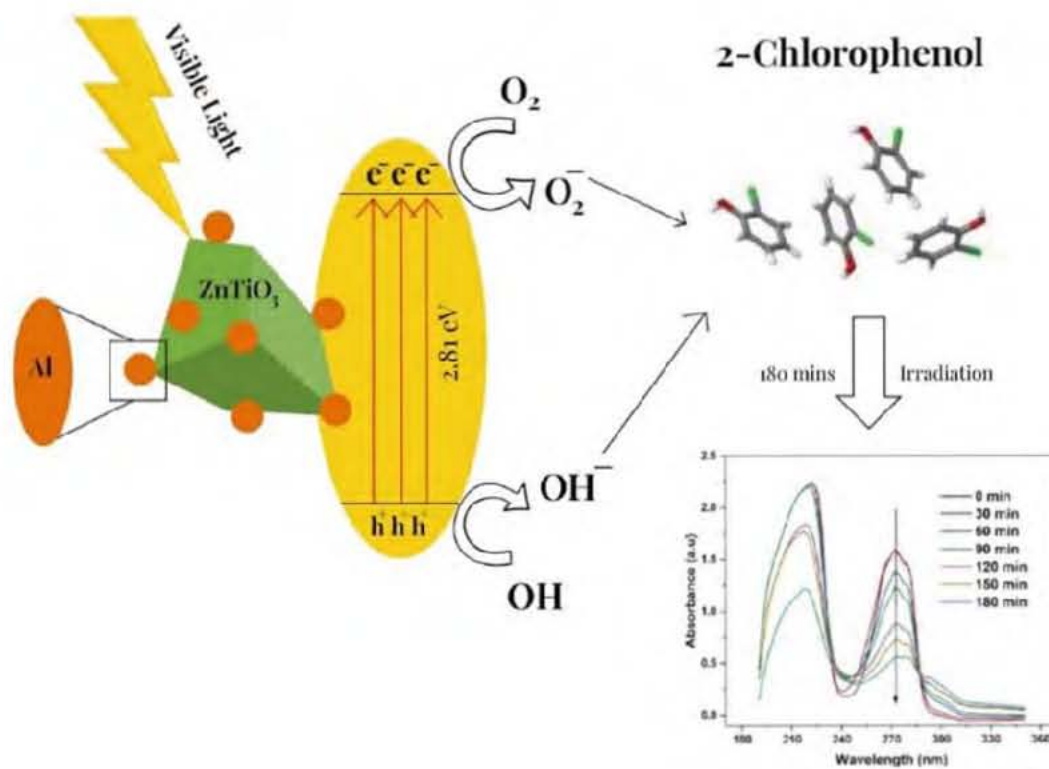
1. INTRODUCTION

1.1. Background

Phenolic compounds are one of the most concerning chemicals in the aspect, that these compounds shows tendency to remain in the surrounding for a longer span of time, remain persistent and have adverse effects on biota (Wu et al., 2021). Natural, industrial, residential, and agricultural activities all contribute to the introduction of phenoplasts into the water bodies as a result of the breakdown or decay of naturally occurring organic substance in aquatic body, as well as dumping of manufactured and domestic pollutants into water bodies and runoff from agricultural and farming regions (Ndebele et al., n.d.). Such compounds tend to change into other chemical substances once they enter the water, which may be more dangerous than the original compounds. The interaction of physical, chemical, biological, and microbiological components in the water causes this chemical metamorphosis.

Phenolic compounds are organic compounds with one or more aromatic rings and one or more hydroxyl groups directly linked to them. Phenol, commonly termed as benzo-phenol, hydroxy-benzene, carbolic acid, is the first chemical in this organic compound series and that is chemically written as C_6H_5OH (Figure 1.1). The other family are made up of phenol derivatives (Pandey et al., 2021).
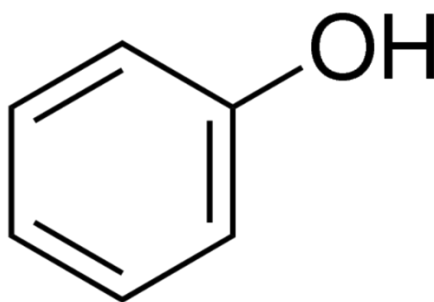
Figure 1.1: Chemical structure of phenols

Due to their hazardous nature and significant short- and long-term impacts on living organisms, phenolic compounds have been designated as pollutants of particular concern by both the US Environmental Protection Agency (USEPA) and the European Union (EU), and have been included in their respective priority lists (Naik & Eswari, 2021). ..As a result, several treatment processes have been developed and are now being used to remove phenol-containing compounds from industrial, household, and urban wastewater before it is

discharged into water bodies. These treatment processes include adsorption, biological degradation, chemical oxidation, and membrane filtration, among others. By using these treatment methods, the harmful effects of pollutants on both terrestrial and aquatic life can be significantly reduced.

Alternative methods for removing phenol-containing compounds from water include extraction, which involves the separation of phenols from water by a solvent; polymerization, which converts phenols into less toxic polymers; and the electro Fenton process, which uses an electrochemical reaction to break down phenols. However, photocatalytic degradation is a promising method because it can effectively remove a wide range of organic pollutants, including phenol-containing compounds, using light and a catalyst.

1.2. Phenolic chemicals reactivity in the aquatic environment

Due to their strong reactivity, phenolic compounds in water are highly prone to interact or react with other components of the aquatic environment, such as inorganic chemicals and bacteria. (Gubin et al., n.d.)

1.2.1. Microorganisms and their interactions

In aquatic environments, certain bacteria can break down uncharged particles, such as alkyl-phenolic compounds, into other phenol-containing resins. However, these new compounds are often more hazardous than the original ones. (Zango et al., 2020).

1.2.2. Inorganic compound interactions

In the aquatic environment, ultraviolet solar energy causes a reaction among phenol and nitrite ions that create $2C_6H_5NO_3$ and 4=nitrophenol in the result. The reaction of the OH^- radical with C_6H_5OH in water produces 2-nitrophenol in a similar way. The presence of NO_3^- ions affects the conversion of C_6H_5OH to $C_6H_5NO_3$. The photo dissociation of phenol in the presence of charge complex made the synthesis of hydroquinone, whereas the addition of Cl in aromatic compounds in water produce C_6H_5CLO. (Gubin et al., 2010). The stepwise reaction is given below:

$C_6H_5OH + HNO_2 + UV \rightarrow 2C_6H_5NO_3 + $ 4-nitrophenol   eq 1.1

$C_6H_5OH + OH- + UV \rightarrow $ 2-nitrophenol   eq 1.2

$C_6H_5OH + NO_3^- \rightarrow C_6H_5NO_3$ eq 1.3

$C_6H_5OH + $ charge complex $ + UV \rightarrow $ hydroquinone   eq 1.4

$$C_6H_5OH + Cl_2 \rightarrow C_6H_5Cl \qquad \qquad \text{eq 1.5}$$
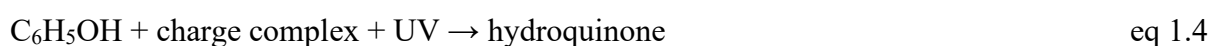
These reactions demonstrate the complex chemistry that occurs when phenol interacts with other components of the aquatic environment under UV radiation.

1.2.3. Phenolic chemicals toxic effect on humans

Phenolic chemicals are known to have a high dermal absorption rate and can be rapidly absorbed from the gastrointestinal tract into the human body. As phenolic chemicals undergo metabolic processes, they are converted into different intermediates such as quinone moieties. These quinones can form covalent connections with biomolecules, resulting in the formation of adducts that cause toxicity in humans. The conversion of phenolic chemicals to quinones occurs through a series of oxidation reactions, which involve the removal of electrons from the phenolic ring and the addition of oxygen atoms to form reactive intermediates called semiquinones. These semiquinones can react further with oxygen to form quinones. (Zhao et al., 2020). 1,2-dichloro-4-(chloromethyl) benzene, 2-amino-1,4-benzenediol, 2,4-dichlorophenol, 4-nitrophenol, and 4-methylphenol (cresol) and other phenolic chemicals are identified harmful to humans. Bisphenol A and certain alkyl phenols have been found to alter the growth of mammary glands in mammals that are exposed to phenolic compounds, resulting in endocrine disruption in humans (Delgado et al., 2020). Bisphenol A has been shown in several studies to postpone the beginning of adolescence in women (Multari et al., 2020). Intake of fluid with higher concentration of phenol, especially drinking water, causes gastrointestinal difficulties as well as muscular tremor and trouble walking (Melati et al., 2020). Catechols can damage DNA or change, degrade various biomolecules present in body, plus impair electron transport in energy transducing membranes because they quickly oxidize to quinone radicals that are most reactive. In the presence of copper, caffeic and dihydrocaffeic acids also damage DNA. Mouth burning, throat burning, and necrotic lesions in the mouth, stomach, and esophagus are all symptoms of chloro-phenol poisoning. It also causes changes in temperature and pulse, as well as weak muscles and convulsions (Cheruvu et al., 2020). Damage to the different body organs are further side consequences of chloro-phenol poisoning (Wang et al., 2020). Chromosomes are also harmed by hydroquinone. Para-cresol and 2,4-dimethylphenol have been classified as chemicals that have the potential to cause cancer.

1.3. 2-Chlorophenol

The choice of 2-CP was decided because 2-CP and its derivatives are common organic contaminants in petrochemical, pharmaceutical, and chemical industry effluent, and if not effectively removed before disposal, they can cause serious environmental concerns.
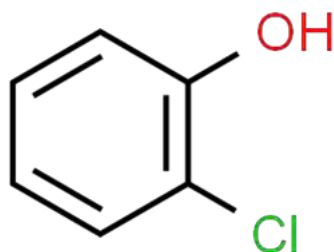
Figure 1.2: Chemical structure of 2-chlorophenol

1.3.1. Hazards summary

2-Chlorophenol (2CP) is a highly toxic and hazardous compound that is commonly used in the manufacturing of pesticides, herbicides, and fungicides. It has been classified as a priority pollutant by the US Environmental Protection Agency (EPA) due to its high toxicity and potential risks to human health and the environment. Exposure to 2CP has been associated with a range of adverse health effects, including irritation of the eyes, skin, and respiratory system, as well as liver and kidney damage. Moreover, 2CP is a known carcinogen and mutagen, with the potential to cause cancer and genetic mutations. Therefore, proper handling and disposal of 2CP and its derivatives are necessary to minimize its impact on human health and the environment.

1.4. Removal of phenolic chemicals from water using various techniques

The removal of phenoplast or phenolic resins from water bodies is required to protect humans and aquatic species from probable contamination with these harmful chemicals. The use of correct methods for efficient cleaning of such substances would alleviate problems connected with pollution and waste disposal and allow the production of value-added phenolic compounds as byproducts. This section describes the available procedures used to successfully remove phenolic chemicals from wastewater.

1.4.1. Ozonation

O_3 is produced naturally when solar UV light penetrates the earth's atmosphere. It forms when hits lightning during a thunderstorm. At high temperatures, oxygen molecules (O_2)

break into $O\bullet$ and then combines with O_2 to form O_3. O_3 with the oxidizing potential -2.74 V than Cl which is utilized for oxidation to remove contaminants from water. Because of its greater oxidation ability, ozone is used as an oxidant to remove organic pollutants from water (Shang et al., 2006).

Ozone is created by sending pure and non-moist air using high voltage O_3 generators, which simulate lightning with corona discharges, or by using UV type O_3 generators to start solar UV rays. The polluted water is to flow beside a vent throat, generating a vacuum that sucks the O_3, or the O_3 is aired up through polluted water. The O_3 then burn and break the pollution causing agents and removed them from H_2O (Shang et al., 2006).

Burning has a high rate of microbe removal, and the bacteria have no chance of acquiring resistance to ozone. Because oxygen from the air is the primary source of O_3, the method is self-stability. Ways to clean biotic, abiotic, and microbiological contaminants from water while also improving its taste and odour (Shang et al., 2006).

1.4.2. Extraction method

One method for removing phenolics from water is extraction, which can be achieved using polar organic solvents. There are two types of extraction methods for phenolic removal from wastewater: liquid extraction and solid phase extraction.

1.4.2.1. The liquid-liquid extraction method

This method divides material into two immiscible liquids based on their solubilities. Normally, the chemicals are divided from one liquid phase to the next. H_2O and organic solvent are the most common immiscible liquids.

The more efficient was found to differ depending on solvent quantity utilized. Aliquot 336 was the best solvent for phenol extraction. Cumene can also be utilized to remove -OH from H_2O. Cumene performed well in an acidic solution for extracting phenol. The dispersion coefficient was found to be related to temperature but reduced when the pH value increased (Sas et al., 2019).

1.4.2.2. Solid phase extraction method

Despite of the efficacy of the liquid-liquid extraction technique for removing substance from polluted water, the approach takes time and is costly, with the risk of injury from the huge number of organic solvents (some of which are poisonous) required in the method. Solid phase extraction that needs less time and organic solvents, is extremely selective, and is

ecologically benign, is thus considered a viable alternative to liquid-liquid extraction (Sas et al., 2019).

In a solid phase extraction device, a needle containing a mixed silica fiber covered with a non-volatile phase is employed. When water solution containing analytes are exposed to the fiber, the analyte builds up on the stationary phase. The filament is then removed from the aqueous solution, and the removed analyte is desorption in a column injection or by gas chromatography (Sas et al., 2019).

1.4.3. Biological methods

The iron oxide nano-particle enhanced solid sucker removed phenol from H_2O with a 98 % efficiency, demonstrating its efficacy (Mulla et al., 2019). Beneath the action of an H donor, one molecular oxygen atoms are reduced to water, and the other O atom is devoured. The synthesis of catechols happens in the next step of the hydroxylation method, which happens when dioxygenase enzyme is present. The conversion of phenol containing compound to chemicals like CO_2 and H_2O occurs after division of the catechol aromatic rings, which occurs at multiple phases with unique enzymes depending on the kind of microorganism (Nthunya et al., 2019). When oxidizing substances like H_2SO_4, HNO_3, and CO_2 or light are present, anaerobic decomposition occurs (Nikolaivits et al., 2019).

In general, the process without oxygen is thought to be suitable for the breaking of phenoplast containing less halogen particles. The anaerobic technique, is best reducing chlorinated phenoplast (Alshabib & Onaizi, 2019). CO_2 and H_2O in the anaerobic system produce methane. When aeration costs are present methane regain, and biomass formation are all advantages of the anaerobic degradation system.

Enzymes, on the other hand, are utilized in the enzymatic way of degradation (biological catalysts). Because enzymes catalyze specific processes at low temperatures, pH, and ionic concentrations, they can be utilized to selectively remove pollutants from water (Campaña et al., 2019). Furthermore, the enzymatic reaction is known to occur at significantly faster rates than other types of reactions (Rahemi et al., 2019). Furthermore, the reaction with enzyme will occur at significantly faster rates than rest of reactions. Biological extraction methods for 2-chlorophenol (2CP) degradation have some limitations, such as slow degradation rates, dependence on environmental factors (e.g., temperature, pH, and nutrients), and limited effectiveness for highly contaminated sites. Additionally, the growth of microbial populations for bioremediation can be affected by the presence of other pollutants or inhibitory

substances in the contaminated environment. These factors can limit the efficiency and applicability of biological extraction methods for 2CP degradation (Sas et al., 2019).

1.4.4. Electro-fenton method

The Fenton reaction occurs when iron (II) reacts with hydrogen peroxide to produce OH•, a nonselective, powerful burning agent. Organic contaminants in aqueous solution have been converted to carbon dioxide and water using this procedure. The Fenton process, on the other hand, has the disadvantages of high reactant costs and dirt production. As a result, a superior technology, the electro Fenton method, has been devised, it has the capability of overcoming obstacles plus allowing improve control of -OH radical formation.

Abdelaziz and team (2009) evaluated the electro Fenton process as a suitable alternative approach for the removal of phenol resin from a phenol tonic polluted water. The electro-Fenton process is an effective method for the degradation of 2-chlorophenol (2CP), but it also has some limitations. One of the main limitations is the high energy consumption associated with the process. The process requires a high voltage to generate the hydroxyl radicals necessary for the degradation of 2CP, which can be energy-intensive and costly (Hao et al., 2021).

1.5. Photocatalytic degradation of phenolic compounds

Semiconductor photocatalytic degradation is a well-known treatment method for wastewater that offers a reliable solution to environmental pollutants and the breakdown of organic pollutants to harmless chemicals like H_2O and CO_2, as well as other species in wastewater. For the breakdown of such organic pollutants, physical, biological and physicochemical water treatments are either inefficient or environmentally incompatible (Barakat et al., 2020).

Photocatalysis use metal oxide catalysts to remove the organic contaminants where the catalyst is mostly activated by the absorption of a sufficient energy photon and can increase the rate of reaction without any wastage. The photocatalytic qualities of metal oxide impetuses are because of the excitation of electrons from the valence to the conduction band of the impetus when it is assaulted with the suitable frequency of light. Electron advancement (e-) causes positive charges or openings (h+) on the valence band, just as electron development on the conduction band of the impetus. The creation of these charge transporters (e-and h+) is the initial phase in the photocatalytic corruption measure. The valence band's pores puncture the oxidized surface, retaining water particles and framing hydroxyl revolutionaries (OH˙). At the point when electrons in the conduction band diminish oxygen

particles, oxygen extremists, otherwise called superoxide revolutionaries ($O^{2\bullet}$), create. These incredibly responsive extremists at that point attack the contaminations, changing them over to innocuous atoms like CO_2 and H_2O (Rashid & Barakat, 2014).
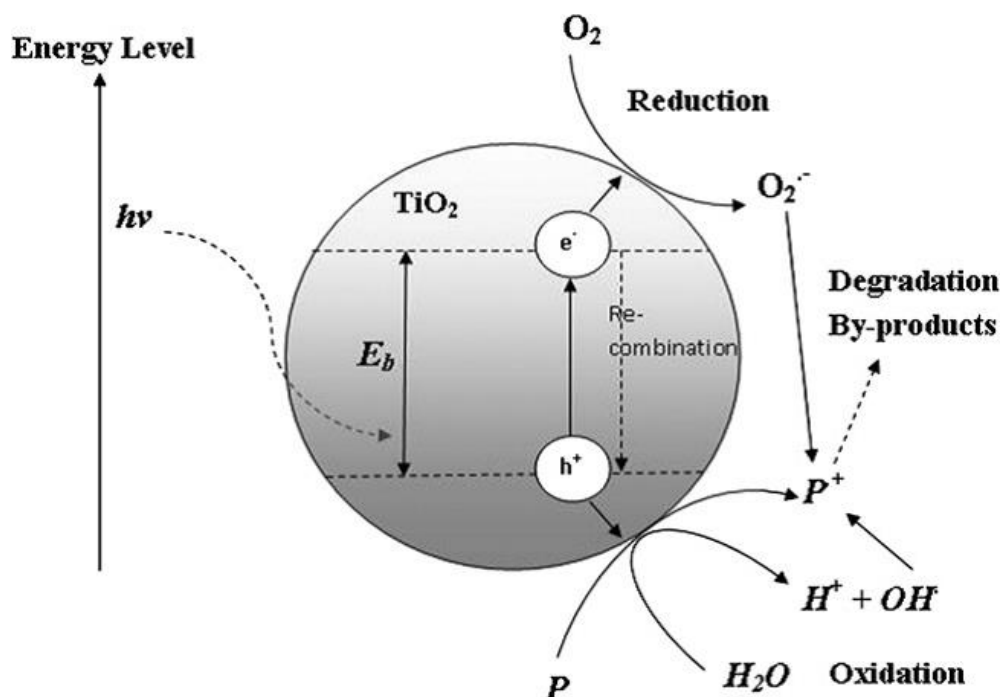
Figure 1.3: General mechanism of photo-catalysis of organic pollutants

Due to its capacity to thoroughly obliterate toxins as opposed to changing them into different items, photocatalytic debasement is perceived as a powerful innovation for eliminating impurities from contaminated water. The success of the degradation process can be influenced by various factors, such as the initial concentration of the pollutant, exposure time, solution pH, and light intensity. Various studies have shown that photocatalytic debasement frameworks may effectively annihilate phenol and its intermediates in water. Mirian and Nezamzadeh Ejhieh, utilized regular clinoptilolite zeolite and FeO-based nanoparticles, under sunlight based light illumination in photocatalytic breakdown of phenol in contaminated water. The outcomes showed that supporting FeO with zeolite improved its photocatalytic corruption effectiveness. The FeO zeolite composite's expanded photocatalytic action was credited to the zeolite's capacity to repress FeO nanoparticle conglomeration and diminish charge transporter recombination. (Rashid et al., 2015).

"Investigated TiO2's photocatalytic degradation potential in the degradation of phenolic chemicals found in refinery wastewater, [the study] discovered that under the conditions of

318 K temperature, pH 3, and a catalyst dose of 100 mg/l, the highest degradation efficiency of phenol and its derivatives was achieved by TiO_2 photocatalysis. At these optimal conditions, a phenol degradation efficiency of 90% was achieved within just 2 hours. The recovery of TiO_2 nanoparticles from filtered water is the main disadvantage of using them for environmental applications. This difficulty can be solved by using magnetic core TiO_2 nanoparticles. Using a range of catalysts, including TiO_2/reduced graphene, ZnO, Fe_2O_3 decorated carbon nanotubes, and CuO, many groups have demonstrated photocatalysis of phenolic compounds. (Barakat et al., 2020; Rashid et al., 2015; Rashid & Barakat, 2014)

1.6. Zinc titanate

The composition of $ZnTiO_3$ is a form of perovskite. It is created by a naturally occurring mineral with the chemical formula of $CaTiO_3$. A general formula for Perovskites ABX_3 with an idealized cubic structure resulted from this. Corner sharing $[BX_6]$ octahedral are found in the ideal crystal structure of cubic perovskite ABX_3. In the Centre of the cube of eight $[BX_6]$ octahedral, the A cation occupy a 12-fold coordination site. The perfect cubic perovskite form is uncommon, and the mineral perovskite is slightly distorted as well. The reduced symmetry of distorted perovskites is an important characteristic for their use as magnetic and electronic materials (Wang et al., 2012).

The blend of a huge oxide particle and a metal particle with a little span shape a cubic close stuffed cross section. Metal particles possess octahedral interstitial positions, near the arrangement of rock salt. At the point when one fourth of the oxygen is supplanted with a cation with a range near that of oxygen, like antacid, salt earth, or uncommon earth components, the measure of octahedral voids filled by a little cation is decreased to one fourth. The substance equation for these materials is ABX_3, and their gem structure is known as perovskite. While oxygen is the most well-known huge particle, other huge particles, for example, F-and Cl-are additionally conceivable (Wang et.al., 2012).

Because of its effective photo-activity, high stability, low cost, and environmentally friendly properties, TiO_2 is the most widely used photo-catalyst. Anatase, on the other hand, is a broad band gap semiconductor with an absorption wavelength of 385 nm. The creation of lower band gap photo-catalysts enabled by visible light is of great interest to allow better use of natural solar energy. Due to its low cost and feasibility, dye sensitization is regarded as an effective technique for extending the photo response to the visible light field. When exposed to natural solar light, sensitized TiO_2 systems exhibit increased photo activity compared to

bare TiO_2 samples (Ajmal et al., 2014). The ZnO-TiO_2 system can take one of three forms: I cubic spinel structures in Zn_2TiO_4; (ii) hexagonal ilmenite structures in $ZnTiO_3$; and (iii) cubic defect spinel structures in $Zn_2Ti_3O_8$ (Wang et al., 2015). The dielectric properties of $ZnTiO_3$ are superior to those of the other two types. The synthesis, however, is difficult because it requires a high temperature and produces large particles with a heterogeneous size distribution (Jaramillo-Fierro et al., 2020).

Zinc titanates have recently been investigated for use in a variety of fields, including paint shade, gas sensor, and reactant sorbent. The relevance of the ZnO– TiO_2 method in practical application continues to attract the attention of researchers. ZnO and TiO_2 are well known for their UV defense and antibacterial properties, but there isn't enough detail about how ZnTiO3 behaves. This piques our attention, so we set out to synthesize the compound and test its antibacterial and UV-protective properties. Specialists are interested in zinc titanate ceramics because of their various applications as paint colors, sorbents, microwave dielectrics, and catalysts. There are a variety of methods for making $ZnTiO_3$ nanoparticles, with the majority of them focusing on solid-state reactions, mechanochemical initiation, and precipitation. The hydrothermal process and the sol-gel method (Chang et al., 2002).

Due to its special properties, such as low-cost materials that are also environmentally friendly, Ti-Zn mixed oxides have potential for photocatalysis applications. high redox potential to push the photocatalysis reaction, chemical and physical stability, non-toxicity, abundance, and various synthesis methods (Gonzales et al., 2021). Pigments, photodetectors, dielectric materials, cameras, and light emitting diodes may all benefit from Ti-Zn mixed oxides. Since their band gap is 3.06 eV, they are widely used for photocatalytic decomposition of organic compounds.

$ZnTiO_3$ was discovered to have photocatalytic and antibacterial properties by researchers. Many studies have shown that $ZnTiO_3$ is stable between room temperature and 945° C, the temperature at which it can split into $ZnTiO_4$ and TiO_2. Meanwhile, fine-tuning photocatalytic behavior requires consideration of processing parameters such as light source and catalyst dosage. The increased photocatalytic activity may be due to the higher reduction-oxidation power, Titania ion coordination, and smaller particle size of the $ZnTiO_3$ calcined at 800 °C (Jaramillo-Fierro et al., 2020).

1.6.1. Photocatalysis mechanism of ZnTiO$_3$

Nanostructured materials dependent on metal oxide semiconductors that are presented to an appropriate sun based light range, like UV or apparent light, can create photo-generated electrons and openings, which would then be able to be changed over to dynamic oxygen species. Its one-of-a-kind property is photocatalysis, which could be used in a wide range of environmental friendly mechanisms. (Nakata & Fujishima, 2012)

Photocatalytic degradation processes have been commonly used in wastewater treatment to destroy organic contaminants. Photocatalysis is an AOP (Advanced Oxidation Process) and it uses a semiconductor along with surface charges to interact with photons and the adsorbed composite via redox reactions, the relationship produces radical species that decays the adsorbed catalyst. Heterogeneous photo-catalysis is commonly used for bleaching and oxidation of dyes and degradation of antibiotics in modern methods. It makes use of the sun's light during semiconductor photocatalysis(Chakrabarti & Dutta, 2004). The radical species formed during the excitation process of semiconductor is mainly responsible for the dye degradation process. (Madhavan et al., 2008). Steps involved in this process are following.

$$Semiconductor + photons\ (hv) \rightarrow e^- (CB) + h^+ (VB) \qquad\qquad eq\ 1.6$$

$$h^+ + H_2O \rightarrow H^+ + OH \qquad\qquad eq\ 1.7$$

$$h^+ + OH^- \rightarrow OH \qquad\qquad eq\ 1.8$$

$$e^- + O_2 \rightarrow O_2^{\bullet} \qquad\qquad eq\ 1.9$$

$$2e^- + O_2 + H_2O \rightarrow H_2O_2 \qquad\qquad eq\ 1.10$$

$$e^- + H_2O_2 \rightarrow OH^{\bullet} + OH^- \qquad\qquad eq\ 1.11$$

$$OP + OH^{\bullet} + O_2 \rightarrow CO_2 + H_2O + other\ degradation\ products \qquad\qquad eq\ 1.12$$
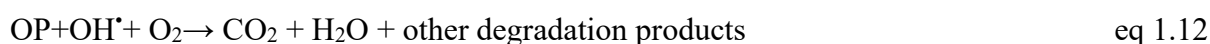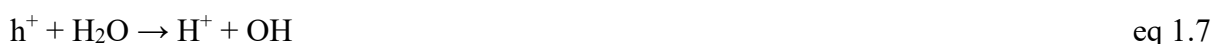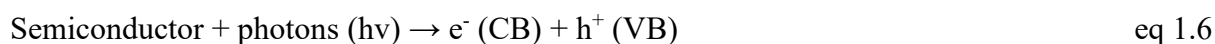
where, OP is organic pollutant.

The presence of a reasonable acceptor (for cb) and benefactor (for vb) once at the outside of the semiconductor will forestall the close to quick and unwanted produced recombination. Conduction-band electrons cb and valence-band openings vb are produced when occurrence photons of energy coordinating or surpassing the semiconductor band-hole energy are consumed by the semiconductor. The presence of a reasonable acceptor (for cb) and contributor (for vb) on the semiconductor's surface will forestall close to quick and unfortunate recombination.

Electron benefactors are hydroxyl anions and water particles adsorbed on $ZnTiO_3$ surfaces, while electron acceptors are atomic oxygen, bringing about the arrangement of hydroxyl ($\bullet OH$) and superoxide (O_2) revolutionaries (Wang et al., 2012). At the point when a natural atom is adsorbed on a semiconductor surface, it goes through a response with the hydroxyl extremist, which is joined by underlying breakdown into numerous intermediates before complete mineralization happens. Photogenerated openings can likewise participate in the immediate oxidation of natural mixtures because of their high oxidation potential (Wang et al., 2012).

Semiconductors consist of excited holes and electrons responsible for degradation of dye. Many semiconductors proved good for degradation and most of them were used in Nano state to enhance the surface area for favorable conditions (Ajmal et al., 2014). In the presence of accelerated environmental contaminant remediation, and it was designed to destroy highly toxic molecules (Gül & Özcan-Yildirim, 2009). The exchange of electrons in the conduction of the semiconductor surface band (generally oxides and sulphides) under particular wavelength illumination is the most common cycle. Superoxide positive ions and hydroxyl radical ions are formed when the produced ions react with oxygen or water. These species can have a high concentration of oxidizing molecules from a variety of industrial dyes (Wang et al., 2012).

1.6.2. Limitations

Photo-catalysts are a promising alternative for wastewater treatment, their recovery at the end of the process limits their realistic application. The photo-catalyst can be held on its surface using the organized supports. As a result, the separation stage is no longer needed. $ZnTiO_3$ has been used in a variety of applications, including gas sensors and photo-catalysis. However, the large band gap of $ZnTiO_3$ (~3 eV) limits its solar energy utilization. The high recombination rate of photo-generated charges, on the other hand, is a limiting factor. Steps must be taken to improve its photocatalytic efficiency (Pirgholi-Givi et al., 2021).

1.6.3. Possible solutions

Various materials that can be used as supports are shown in the literature. Silica, ash, zeolites, active carbon, clays, and aluminum are among them. Aluminum may be a viable option. Chemical and mechanical stability are high in these materials. Aluminum is an affordable material that offers a unique opportunity to create value from local resources.

One feasible and practical approach is to form a heterojunction structure by coupling $ZnTiO_3$ with a kind of narrow band gap semiconductor. The narrow band gap semiconductor may act as a sensitizer, increasing photocatalytic efficiency and light harvesting capacity. Due to changes in surface polarity, the generation of additional defects, and changes in growth orientation, doping may cause changes in the host's morphology.

1.6.4. Metal and non-metal doping

Heterogeneous photo-catalysis with suspended $ZnTiO_3$ is of particular interest due to the photo-catalyst's chemical stability and low cost. Doping can change morphology, nanoparticle growth orientation, surface polarity and can create additional defects. Because of their numerous applications in catalysis, doped zinc titanates have sparked a lot of interest (Gao & Qu, 2020).

Table 1.1: Comparison of activity of different titanates on organic pollutants

Catalyst/Heterojunction	Dopant name and Concentration	Preparation Method	Application	Light source	Reference
$ZnTiO_3$	Non doped	Hydrothermal and Sol Gel	95% degradation of Methyl Orange	UV	(Yan et al., 2015)
$ZnTiO_3$	2% Lanthanum doping	Sol Gel method	90% degradation of Rh B	Visible	(Abirami et al., 2021)
$ZnTiO_3/Zn_2Ti_3O_8/ZnO$	Non doped	Solvothermal-calcination method	30% degradation of phenol	UV	(Chen et al., 2020)
$TiO_2/ZnTiO_3/\alpha Fe_2O_3$	Non doped	Sol Gel method	90% and 80% degradation of methylene blue and methyl orange respectively	UV	(Online et al., 2014)i
$ZnTiO_3$	Non doped	Sol Gel method	70% degradation of Methyl Orange	UV	(Perween & Ranjan, 2017)
$ZnTiO_3/SiO_2$	Non doped	Sol Gel Method	91% of Red X-3B	UV	(Chen et al., 2020)
ZnTiO3	0.02% Ag-Fe co-doped	Sol Gel method	93% degradation of Methylene Blue	UV	(Abirami et al., 2021)
TiO_2	1% Al doped	Solvothermal Method	80% degradation of norfloxacin	Visible	(Kaushik et al., n.d.)

Various metallic and non-metallic dopants were observed to cause shift inside the absorption band closer to visible light vicinity especially for metal ions along with V, Cr, Mn, Fe and Ni, there was an explosion of interest in $ZnTiO_3$ doping with non-metal ions (e.g. N, C, S, F).

Nitrogen is considered as one of the simplest non-metal ion dopants for $ZnTiO_3$. Optical absorption of the N-doped $ZnTiO_3$ was extensively improved inside the visible light location with a wavelength less than 500 nm compared to the authentic $ZnTiO_3$. Improvement on photocatalytic efficiency became additionally located inside the degradation of numerous contaminants under visible light irradiation (Conesa, 2013).

1.6.5. Aluminium doping

Aluminum doping was done because holes are the majority carriers and will enhance oxidation capacity of titanates. Hence doping of p-type materials may increase the photo-oxidation efficiency of a semiconductor. Aluminum upgrades photo-chemical charge partition in strontium titanate photocatalysts in general water parting (Zhao et al., 2019). Using Photocatalysis of natural contaminations from wastewater utilizing aluminum doped TiO_2 was done in an investigation. The evacuation of natural toxin by TiO_2/doped with Al was 80% at a measurements of 0.5 g/L and was 85% at a dose of 1 g/L. A significant decrease of norfloxacin adsorption was appeared by 1% A-T, which was around 209 mg/g. Al Doped TiO_2 impetus (1% AT) shows an around multiple times higher rate steady towards the norfloxacin evacuation than non-doped (Zhao et al., 2019).
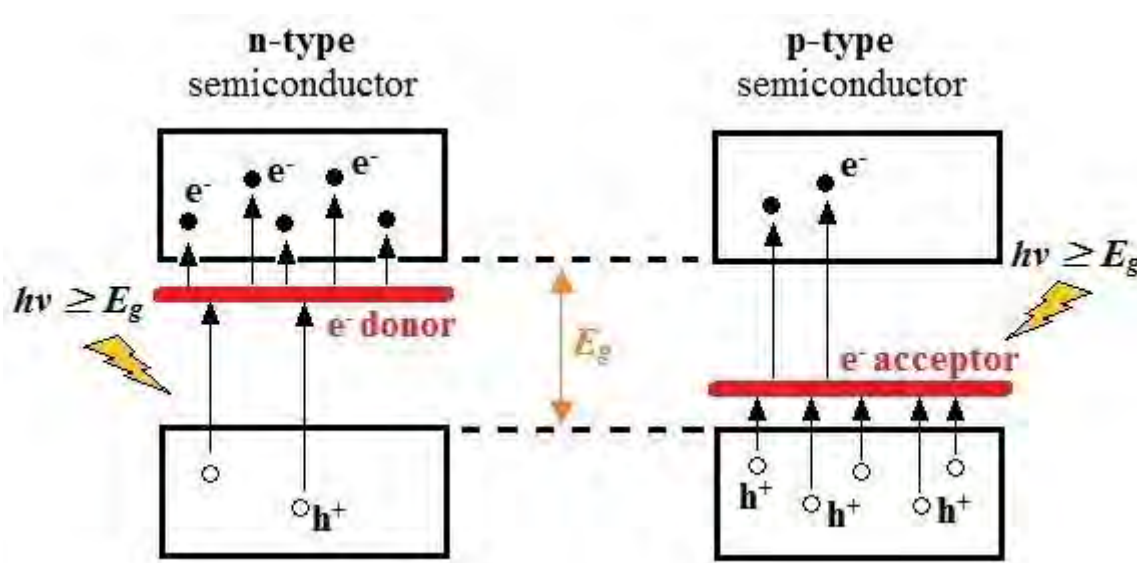

Figure 1.4: Illustration of n-and-p type semiconductors

1.7. Parametric factors affecting rate of photocatalytic degradation

1.7.1. Catalyst loading

One of the most crucial parameters of photocatalytic degradation is catalyst loading. The rate of photocatalytic degradation of organic pollutants increases when active sites increase with

photocatalytic dosage. In this process hydroxyl radical production increases from irradiated photo catalysts. At low catalyst loading degradation decreased this happens because of more light transmitted through the reactor and lesser transmitted radiation only will be used in the photocatalytic reaction. When the catalyst loading exceeds a certain limit, the degradation process may be reduced as the suspension becomes more opaque, causing an increase in light scattering and a decrease in photon penetration depth, resulting in fewer activated photocatalysts (Kumar, 2017).

1.7.2. Initial concentration of pollutants

Concentration is a crucial parameter which affects photocatalysis. Initially, when the number of pollutants is low the reaction will be fast at optimum conditions but the speed of reaction is inversely proportional to initial concentration of the pollutants because an increase amount of pollutants cause deficiency of active sites on enzymes and due to unavailability of catalyst surface generation of ROS (Kumar, 2017).

In this way, due to enhanced concentration of pollutants overall catalytic surface use is reduced. 4-chlorophenol The degradation of certain organic compounds by photocatalysis may require a longer illumination time due to the formation of intermediate products, as compared to oxalic acid which undergoes direct mineralization to CO2 and H2O (Kumar, 2017).

1.7.3. Effect of pH

pH is the most important parameter that can directly affect the rate of photocatalytic degradation. A slight change in the pH of any photocatalytic reaction can trigger the reaction in a reversible direction thus decreasing efficiency.. Low pH means the amount of Hydrogen ions are more in number. High pH shows the number of hydroxyl ions are more in concentration in the solution. For example, a study has shown that changes in pH can affect the surface charge of titania and alter the probability of collaborative reactions. Under acidic or basic conditions, the surface of titania can be protonated or deprotonated, respectively, as indicated by the following reactions. (Kumar, 2017).

$TiOH + H \rightarrow TiOH_2$ eq 1.13

$TiOH + OH \rightarrow TiO + H_2O_2$ eq 1.14
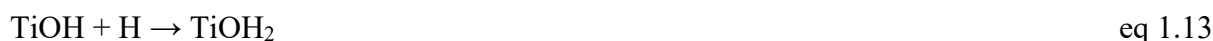
1.7.4. Reusability of catalyst

Catalysts are reusable because they can trigger a chemical reaction without being consumed during the reaction. But the catalytic activity or efficiency of catalysts decreases with the passage of time due to several reasons like loss of active sites, accumulation of reactants and products on the catalyst surface, etc, and aging process is one of them. Catalysts can lower the activation energy of a chemical reaction by providing an alternative reaction pathway with lower energy requirements. However, in photochemical degradation reactions, the activation energy is primarily provided by the energy of the incident light, which is not affected by the catalyst. Therefore, the catalyst can only facilitate the reaction by increasing the probability of reactant molecules coming into contact with each other on its surface, but it cannot lower the activation energy of the reaction at the same level as in traditional chemical reactions (Kumar, 2017).

So, the reusability of the catalysts is not unlimited, it has a specific time range after which they cannot help in a chemical reaction with the same efficiency. To understand this, let's consider an example of trans-esterification reaction under optimal conditions of 12:1 methanol: oil molar ratio, 4 wt% catalyst, and 3 hours of reaction time. The catalyst was reused for subsequent trans-esterification runs under the same conditions. It was observed that the conversion of RSO to biodiesel was 99.6% in the first run before catalyst recovery, but it decreased to 86.4% after the seventh recovery run. This decrease in efficiency can be attributed to several factors, such as catalyst deactivation due to fouling or poisoning, loss of active sites on the catalyst surface, and changes in the catalyst's physical and chemical properties during reuse. These factors collectively reduce the catalyst's ability to lower the activation energy of the reaction, leading to a decrease in efficiency over time (Kumar, 2017).

1.8. Problem statement

Conventional treatment approaches are ineffective at removing CP from the environment, instead causing the creation of more harmful chemical compounds. Photo-catalysis is often considered a promising solution to address the issue of wastewater contamination, as it is an advanced oxidation process that can effectively eliminate harmful organic compounds. However, due to the huge energy band gap (3.2 eV), it can only be used for UV photo-catalysis that is about 4% of the solar spectrum incident on Earth. TiO_2 alone is unsuitable for visible light activated photo-catalytic applications because of this reliance. Also, most often utilized photo-catalysts are either poisonous, expensive, or many of them have recombination concerns.

To fill these gaps, researchers produced modified photo-catalysts that can harness the visible spectrum of light, which makes up the majority of sunlight (46 percent). Different doping and heterojunction materials with better photocatalytic capabilities, as well as nontoxic and chemically stable compounds, are created for this purpose. Further, at the nanoscale, various 1D and 2D nanostructures have been developed, each with unique properties.

1.9. Aims and objectives

1. Hydrothermal synthesis of titania nanotubes
2. Sol-gel synthesis of zinc titanate
3. Doping of $ZnTiO_3$ with different percentages of Aluminum (1% and 3%)
4. To check the efficiency of proposed system to remove 2-CP from synthetic wastewater
5. To check effects of pH, catalyst dose and pollutant concentration on the activity of 1% $Al-ZnTiO_3$
6. Check the reusability of 1% $Al-ZnTiO_3$
7. Mechanism study by using scavengers, of 2CP using 1% $Al-ZnTiO_3$

2. MATERIALS AND METHODS

2.1. Chemicals and reagents

Sodium Hydroxide (NaOH) pallets, Titanium (IV)s oxide - Anatase, Zinc Nitrate (hydrate), Aluminum Nitrate Nona hydrate precursors were used for the preparation of nano composites. 2-Chlorophenol was target pollutant used for degradation while 0.1M HCl and NaOH were used for maintaining pH of reaction. All the chemicals used were of analytical grade.

2.2. Synthesis of nanocomposites

2.2.1. Hydrothermal synthesis of titanate nanotubes

Hydrothermal synthesis was used for the preparation of TNTs.10M solution of NaOH was prepared by adding 44g of NaOH in 110ml of distilled water. 2g of Titanium oxide (Anatase) added to the NaOH solution and their mixing is done through continuous stirring for one hour. The solution is then placed in teflon-lined autoclave (Volume 45cm^3, 80% filled)

Hydrothermal synthesis was performed at the temperature of 180°C for 20 hours. As obtained product is isolated and then washed with distilled water until its pH reaches 8. To make titania nanotubes protonated, the powder was washed with excess of 0.1M HCl for more than 30 min until it reaches pH 2. Then water washing was done to reach the value of pH 5. The obtained sample was dried at 140°C for 12 hours. The obtained powder were grounded and stored. (Wang et al., 2015).

Figure 2.1: Synthesis scheme of titania nanotubes
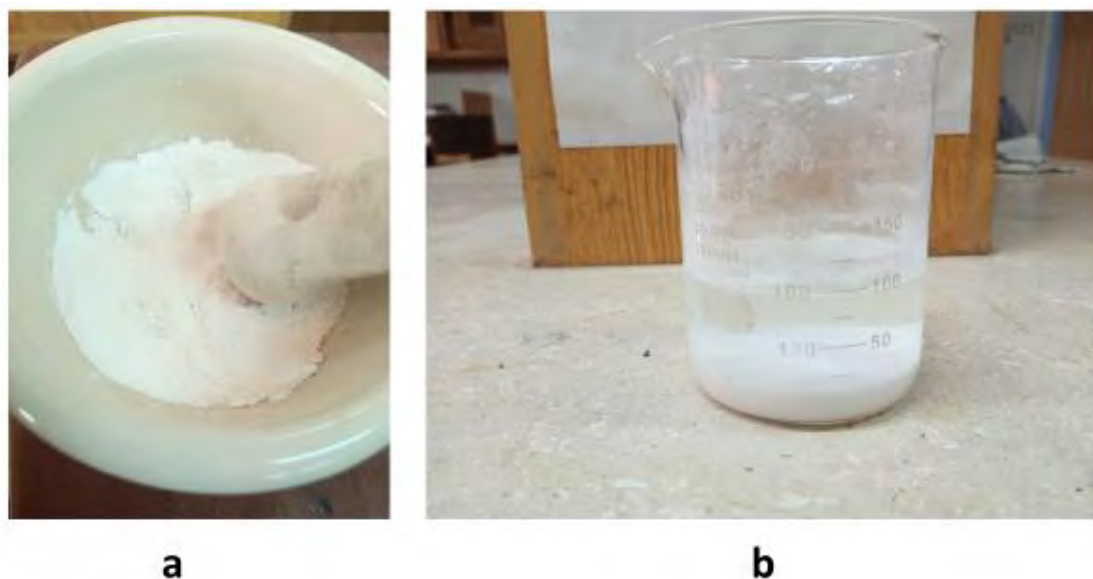
Figure 2.2: (a) Titanate nanotubes **(b)** Washing of titanate nanotubes with deionized water.

2.2.2. Synthesis of ZnTiO$_3$ by sol-gel method

$Zn(NO_3)_2H_2O$ and the obtained titania nanotube powders were added in water in the stoichiometric ratio to form a solution. The solution was continuously stirred, and its pH was adjusted to 6. After that it's heated to 80 °C for 2h. The precipitates obtained washed with DI several times to avoid the adsorption of Zn^{2+} and NO_3^-. The product made was filtered and then dried. After that calcination at 700 °C was done for 3 hours in air. Catalyst powder was obtained after grinding (Yan et al., 2015).
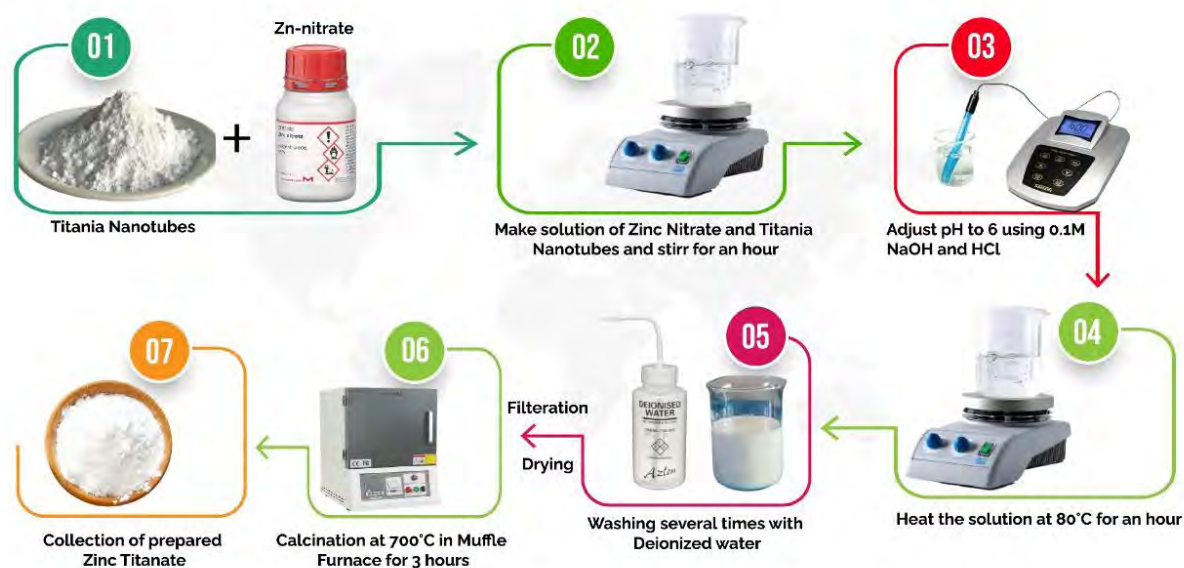
Figure 2.3: Synthesis scheme of zinc titanate

Figure 2.4: Calcined ZnTiO₃

2.2.3. Synthesis of Al doped ZnTiO₃

To check which percentage of doping will perform best we prepared 1, 3 and 5 % aluminum doped Zinc titanates. To synthesize Al-ZnTiO₃, we took the above-mentioned amount of as prepared ZnTiO₃, it was as sonicated in 30 mL of DI, then added to the solution containing specified Aluminum nitrate nonahydrate. It was kept on continuous stirring to form gel at 90°C. Finally, the as obtained gel was calcined at 700°C for 1 hour in a conventional furnace in air. After calcination, it was allowed to cool at room temperature and the prepared powder was collected. (Gholami et al., 2017).
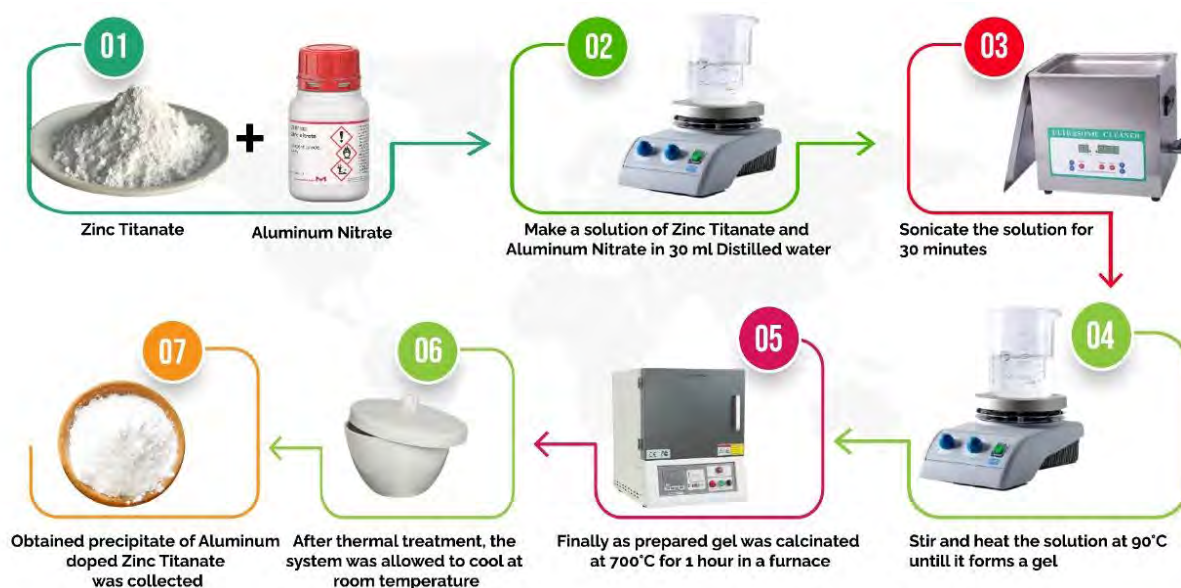
Figure 2.5: Synthesis scheme of Al-ZnTiO₃
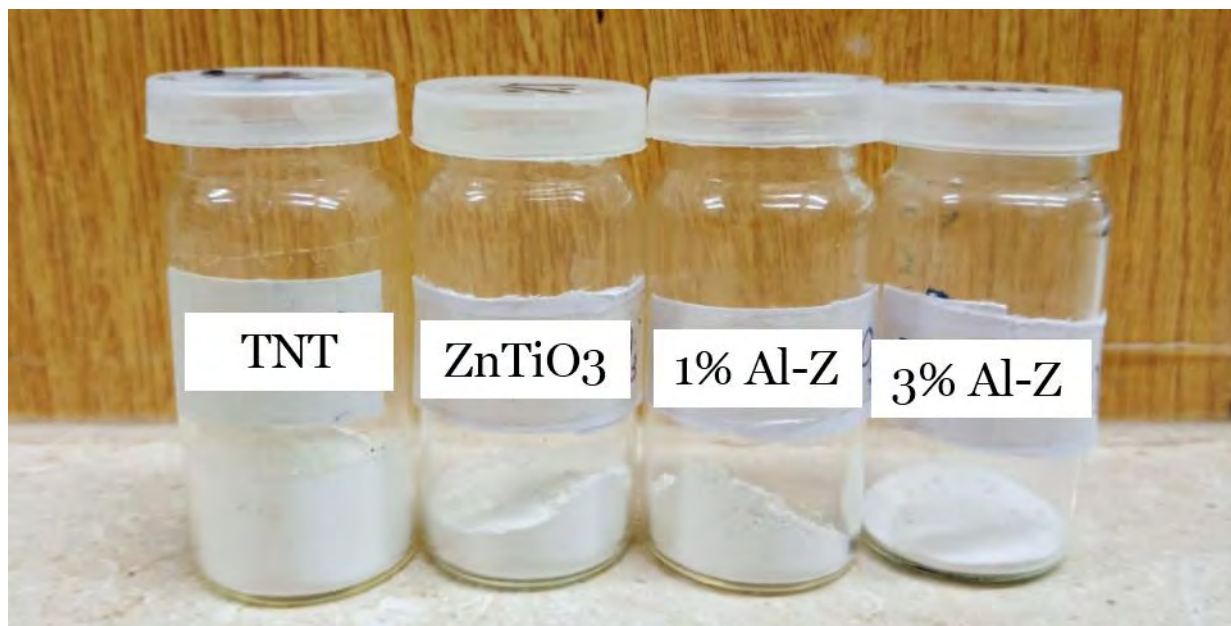
Figure 2.6: Prepared Titania nanotubes, $ZnTiO_3$ and aluminum doped $ZnTiO_3$ (1%, 3%) powders

2.3. Standard stock solution preparation

First, preparation of 100 ppm stock solution of 2-CP was prepared using certain stoichiometric concentration of pure 2-CP. Pure 2-CP was dissolved in 1000 ml deionized water in conical flask with continuous magnetic stirring for 12 hours as 2-CP slowly dissolves in water. All working solutions were prepared from stock using the following dilution formula.

$$C_1V_1 = C_2V_2 \hspace{6cm} \text{eq 2.1}$$

2.4. Adsorption

Adsorption experiment of 50 mgL^{-1} 2-CP solution was conducted by adding 0.5gL^{-1} of 1% Al-$ZnTiO_3$. The solution was placed in dark for 3 hours at pH = 8. Activity was observed by taking 4-5 ml aliquots of reaction mixture using syringe after every one hour. The samples were later filtered using 0.22-micron syringe filters (Khezami & Capart, 2005).

2.5. Photolysis

Photolysis experiment was conducted using 100 mgL^{-1} of 2-CP of 1% Al-$ZnTiO_3$. The solution was placed in direct sunlight for 3 hours. Activity was observed by taking 4-5ml aliquots of reaction mixture using syringe in amber glass bottles (Srivastava et al., 2010).

2.6. Photocatalytic reactions

The photodegradation of 2-CP solutions was carried out in a 250ml beaker under solar light. 100 mgL^{-1} stock solution was prepared by using distilled water in continuous stirring for 24 hours. 50 ml solutions of 2-CP in different concentrations (20, 50, 75 and 100 mgL^{-1}) were placed in a beaker and then photocatalyst (0.l, 0.25, 0.5, 0.75, 1, 1.5 gL^{-1}) was added. Prepared Titania nanotubes, Pure $ZnTiO_3$ along with all aluminum dopants were used in experiments. Before taking solution to solar irradiation, it was magnetically stirred in dark for 30 minutes to maintain adsorption-desorption equilibrium. Then reaction was placed in direct sunlight covering the beakers with watch glass. At every 30 minutes time intervals, 4-5 ml samples were taken in amber glass bottles using syringe and particles were filtered using 0.22-micron syringe filters.

Figure 2.7: Photocatalysis under direct sunlight

The samples were later analyzed using UV-Vis Spectrophotometer and the results were analyzed. Degradation efficiency of all samples was calculated using following equation.

Percentage Degradation = (initial conc. – final conc.) / (initial conc.)×100   eq 2.2

2.7. Analysis by UV-visible spectrophotometer

All the samples taken during the experiment were analyzed by UV-Visible spectrophotometer. Absorbance of all samples was taken on 274 nm where the highest peak

was located (Sharma et al., 2019). Abundance was noted and the concentrations of all samples were assessed by equation as follows;

y= mx$\pm$ c   eq 2.3

Where **y** is absorbance (arbitrary unit)

m is intercept

c is slope

x is concentration of target analyte

2.8. Parametric studies of photocatalysis

2.8.1. Initial concentration of 2CP

Initial concentration of pollutant is very important parameter which explains that how the increase and decrease in initial concentration of pollutant effect the photocatalytic degradation. The experiments were performed on 20 mgL^{-1}, 50 mgL^{-1} and 100 mgL^{-1} of 2CP to find out optimum pH where the efficiency was maximum. All experiments were performed under same conditions (pH = 6, catalyst dose = 0.5gL^{-1}) (Rashid & Barakat, 2014).

2.8.2. Effect of catalyst loadings

To find out optimum catalyst amount successive experiments were performed using different catalyst amount of 0.1 gL^{-1}, 0.25 gL^{-1}, 0.5 gL^{-1}, 0.75gL^{-1}, 1gL^{-1}, 1.5gL^{-1} under same conditions (Initial Concentration = 100 mgL^{-1}, pH = 6, irradiation time = 180 min) (Yan et al., 2015).

2.8.3. Effect of solution pH

Solution pH has proved as one of the most crucial factors that influence the degradation of organic pollutants. To find out optimum pH series of experiments were performed using several pH of pH 2, pH 4, pH 6, pH 8, pH 10 under same conditions (Initial Concentration = 100 mgL^{-1}, catalyst dose = 0.5 gL^{-1}, irradiation time = 180 min)

2.8.4. Point of zero charge (PZC)

Point of zero charge is another important factor to check the surface charge of catalyst. PZC is the pH of our catalyst where it behaves normal. Above PZC, catalyst surface is negative charged and below PZC it is positively charged. PZC of catalyst was calculated by salt addition method. 0.1M KCl was taken in 5 beakers and their pH was maintained at 1, 3, 5, 7, 9 and 11 by utilizing 0.1M of HCl and then NaOH. After pH adjustment 0.5 gL^{-1} amount of

catalyst was added in all beakers and left them for 24 hours. After 24 hours final pH readings were taken, and graph was plotted between initial and final concentrations to get the value of PZC (Rashid & Barakat, 2014).

2.8.5. Reusability

Reusability of catalysts don't mostly decline the activity of catalyst. Series of experiments were performed by using the filtered catalyst after washing simply with water. All the experiments were done under same conditions (2-CP concentration = 100 mgL^{-1}, Catalyst dose = 0.5 gL^{-1}, pH = 6) (Harifi & Montazer, 2014).

3. RESULTS AND DISCUSSION

3.1. X-ray Diffraction

Fig. 3.1 shows patterns of prepare $ZnTiO_3$ and Al doped $ZnTiO_3$ nanocomposites after calcination at 700ºC. The appearance of the prominent peaks at 30.032, 35.379, 38.7 and 62.44 are attributed to the Miller-Bravais indices of (2 2 0), (3 1 1), (3 2 0) and (4 4 0) respectively. These crystallographic planes are matched with PDF# 39-0190 representing $ZnTiO_3$. The phase is pure with cubic cells and unit cell parameters are a=8.408, α= 90º and V=594.4Å. while diffraction peaks at 2θ values at 25.281, 36.946, 37.800, 38.575, 48.049, 53.890, 55.060, 62.119 and 75.029 corresponds to (1 0 1), (1 0 3), (0 0 4), (1 1 2), (2 0 0), (1 0 5), (2 1 1), (2 1 3) and (2 1 5) crystallographic planes are perfectly matched with JCPDF card No. 21-1272 representing protonated Titania nanotubes used for preparation of $ZnTiO_3$. Intensity of Characteristic peak of titania is increased with formation of $ZnTiO_3$ and is reduced with intrusion of Al as dopant. Moreover, XRD patterns of 1% Aluminum doped $ZnTiO_3$ shows Alumina's characteristic peak at 44.7º attributed to (4 0 2) crystallographic plane, which is matched with JCPDF# 04-0787. While intensity of this peak reduced with the increase in doping percentage as shown in Fig. 3.1.

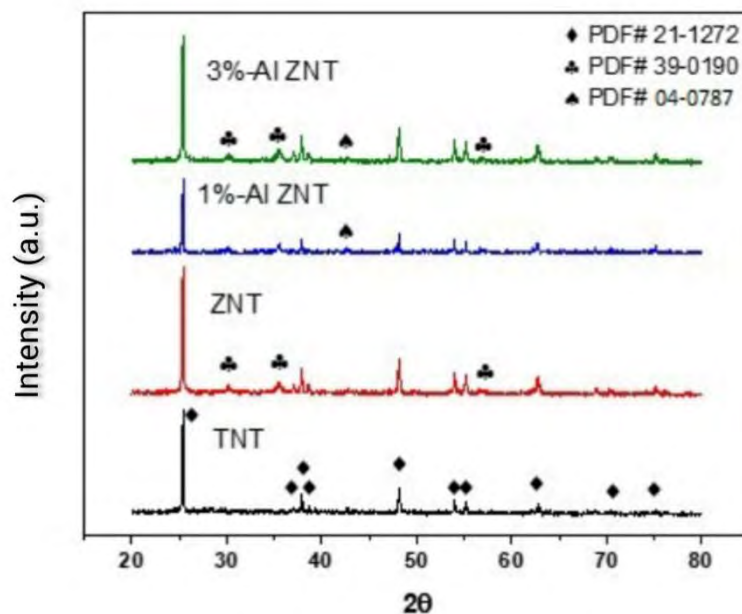**Figure 3.1:** X-ray Diffraction analysis

3.2. Photoluminescence

The photocatalytic degradation of the $ZnTiO_3$ and Al-$ZnTiO_3$ could be explained by the PL spectra. Photoluminescence explains the recombination processes of photo-induced electron-

hole pair, their migration and transfer in semiconductor materials. The spectra of as prepared Titanate nanotubes, $ZnTiO_3$ and Al-$ZnTiO_3$ were obtained at room temperature with excitation wavelength of 285 nm. It can be seen that all the samples have a strong peak around 577 nm in the spectrum. Interestingly, the PL intensity has greatly decreased, showed significant reduction in the recombination rate of the photo-induced electron and hole pairs in 1% Aluminum doped $ZnTiO_3$ nanoparticles. The highest reduction in recombination rate has been observed in 1% Al-$ZnTiO_3$ (Fig. 3.2).
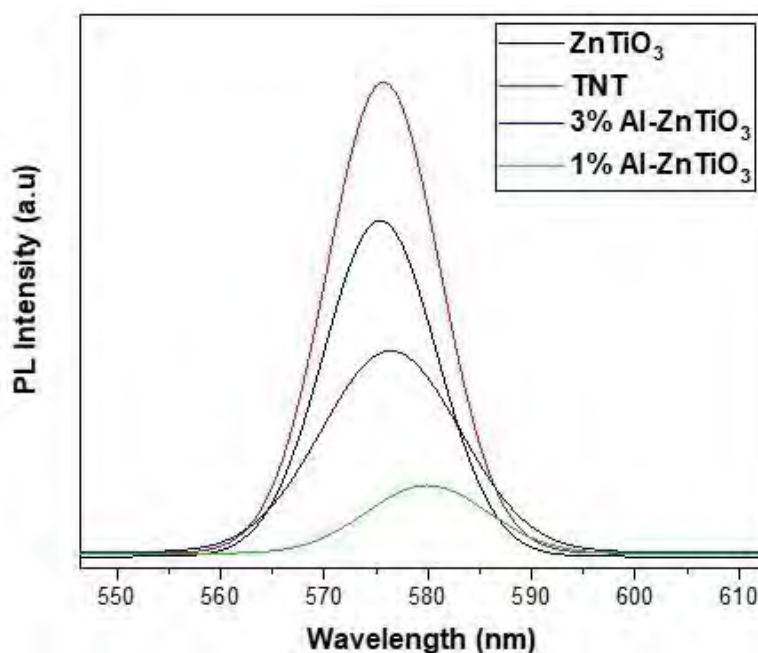
Figure 3.2: Room temperature photoluminescence (PL) spectra of the synthesized non-doped, Al-doped $ZnTiO_3$ and Titania nanotubes

3.3. UV-Vis Diffuse Reflectance Spectra (DRS)

The electronic and optical properties of the samples were analysed by UV-Vis diffuse reflectance spectroscopy. For titania nanotubes and $ZnTiO_3$ a sharp peak was observed at 350-400*nm*. Doping of $ZnTiO_3$ with the aluminum caused a sharp decrease in reflectance and a shift of peak towards the visible. The spectrum suggested that prepared aluminum doped $ZnTiO_3$ are more visible light active as they show reflectance peak in visible region greater than 400 nm. Reflectance shown in visible region of the AL-$ZnTiO_3$ is because of the electron donor fermi levels formed by the aluminum doping in the crystal lattice of $ZnTiO_3$. As aluminum doping introduced more p-type charge carriers in system of $ZnTiO_3$, so it created the fermi levels on the respective band (Surendar et al., 2014).
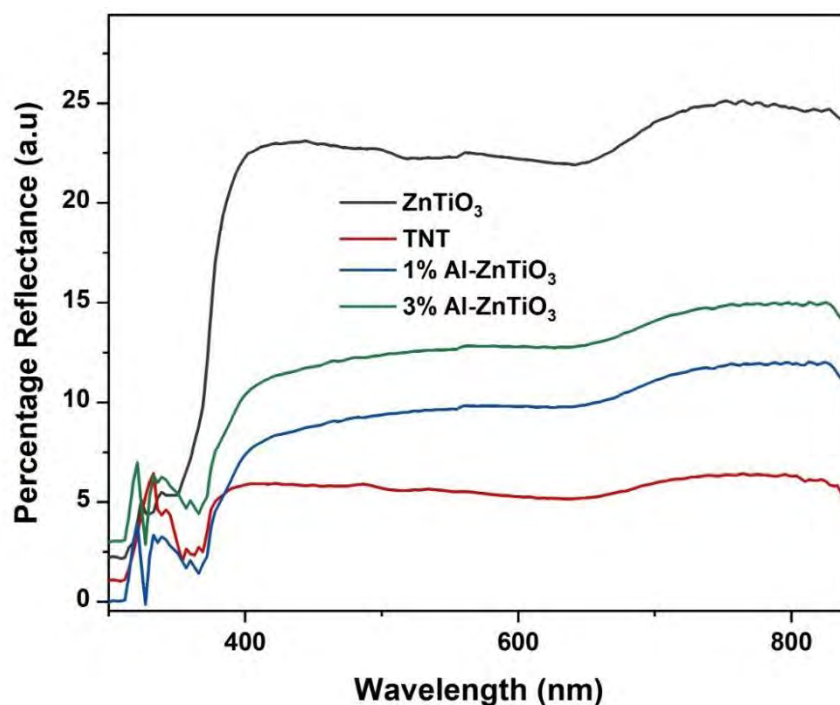
Figure 3.3: UV-Vis DRS of $ZnTiO_3$, Titania Nanotubes, 1% Al-$ZnTiO_3$ & 3% Al-$ZnTiO_3$

Kubelka equation was used here to calculate the band gap of as prepared catalysts. UV-Vis DRS data is used in the equation for calculation. Equation is as follows:

$$F(R) = (1-R^2)/2R \qquad\qquad\qquad\qquad\qquad\qquad\qquad \text{eq 3.1}$$

$$F(R) \times hv = B(hv - Eg) \qquad\qquad\qquad\qquad\qquad\qquad \text{eq 3.2}$$

Where FR is Kubelka Munk Function, *hv* is Energy of one photon and its value can be calculated by $1240/\lambda$. Eg is band gap of sample that can be calculated from above equation. Plotting value of $(FR \times hv)^2$ on Y-axis and *hv* on X-axis and a peak is obtained as in Fig. 3.3. A projection was drawn to calculate exact band gap of all the prepared samples by UV-Vis DRS data in Fig. 3.3.
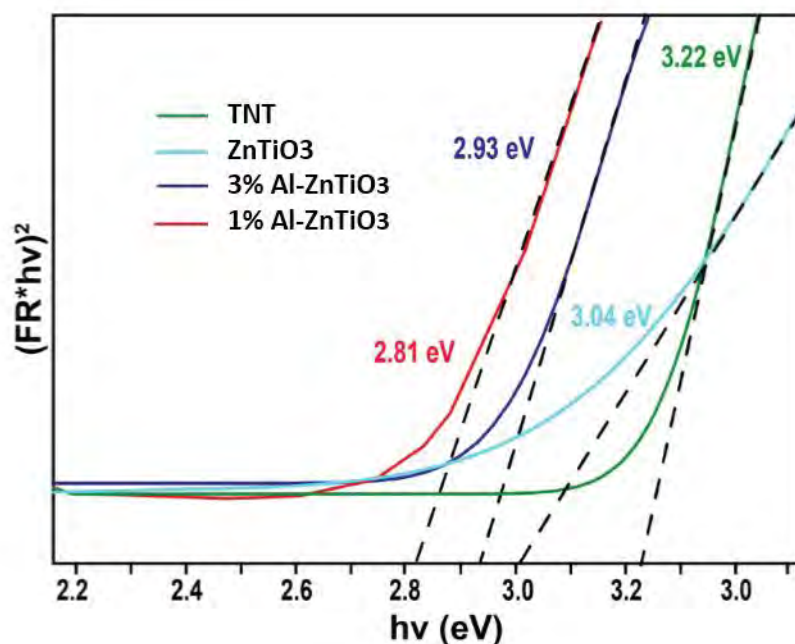
Figure 3.4: Band gap of as prepared samples (TNT, $ZnTiO_3$, 1% Al-$ZnTiO_3$, 3% Al-$ZnTiO_3$)

The band gap of 1% Al-$ZnTiO_3$ and 3% Al-$ZnTiO_3$ comes out to be 2.81 eV and 2.93 respectively. It shows that as we increase the doping percentage of aluminum in $ZnTiO_3$ the band gap increases. Band gap of $ZnTiO_3$ reported in literature is 3 eV (Yan et al., 2015) and that of TiO_2 is 3.2 eV. So the band gap of aluminum doped $ZnTiO_3$ showed that sample is visible light active and also lowers rate of recombination (Fig 3.5).

3.4. Degradation of 2-Chlorophenol by different catalyst

The photocatalytic efficiency of 2CP was analyzed by using titanate nanotubes, pure $ZnTiO_3$ and its aluminum dopants (1% and 3%) as shown in Fig. 3.7. Photocatalytic degradation of all the catalysts were done using initial concentration of 100 mgL^{-1} 2-CP, 0.5 gL^{-1}. The pollutant 2CP used had normal solution pH (pH=6) with the illumination time of 180 minutes in direct sunlight. The descending order of the degradation is given as 1% Al-$ZnTiO_3$ > 3% Al-$ZnTiO_3$ > Pure $ZnTiO_3$ > TiO_2 nanotubes and 81.60 > 76.37 > 70.34 > 52.79 respectively as shown in Fig. 3.7. All samples were investigated on UV-Visible Spectrophotometer. Maximum wavelength selected was 274 nm. Standard calibration curve and linearity was achieved efficiently as Coefficient of determination (R^2) was 0.9997 as shown in Fig. 3.5.
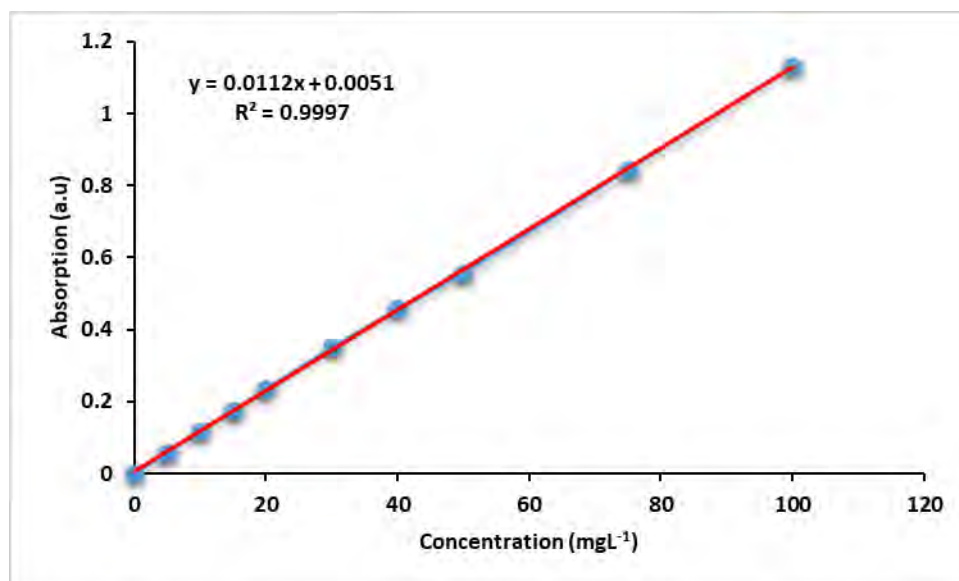
Figure 3.5: Standard calibration curve

Before putting experiments in direct solar radiations, catalyst was added into the solution having the pollutant and placed in dark to get adsorption-desorption equilibrium. This was found to be very less as compared to photocatalytic degradation. Also 180 minutes adsorption and photolysis (without catalyst) experiments were done with all catalysts and both experiments showed minimum activity as compared to photocatalysis as shown in Fig. 3.6.
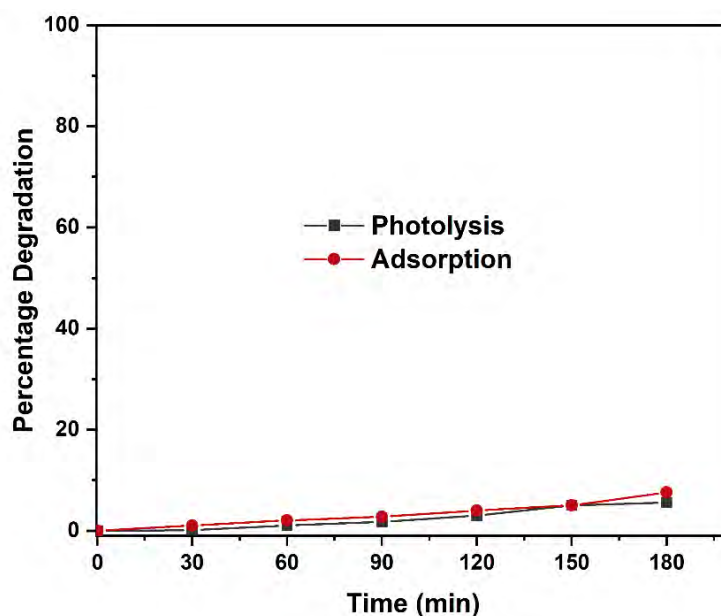
Figure 3.6: Photolysis of 2CP without catalyst (pH=6, 2CP concentration = 100mgL^{-1}) (b) Adsorption of 2CP in dark (pH=6, 2CP concentration = 100 mgL^{-1}, Catalyst dose = 0.5 gL^{-1})
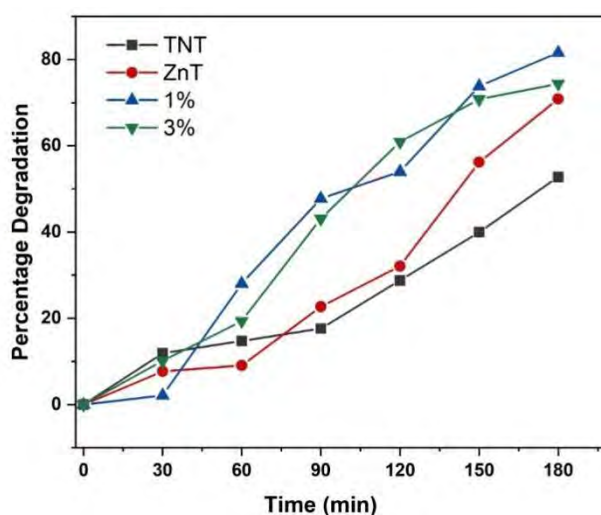
Figure 3.7: Effect of different catalysts (ZnTiO$_3$ and its dopants) on 2-Chlorophenol degradation efficiency under solar radiation (Catalyst dose = 0.5gL^{-1}, 2-Chlorophenol concentration = 100 mgL^{-1}, irradiation time = 180 minutes)

3.5. Effect of Catalyst Dose

Catalyst dose effect is one of the most important parameters that influence photocatalysis. Series of experiments were organized to find out optimum dose of catalyst for efficient photocatalysis. Different catalyst dose from 0.1 gL^{-1} to 1.5 gL^{-1} were selected under same conditions (Initial concentration = 100mgL^{-1}, pH = 6) for 180 minutes under direct sunlight. The degradation efficiency of all the catalysts is shown in Figure **3.8.** The degradation of 2-CP at 0.1 gL^{-1}, 0.25 gL^{-1}, 0.5 gL^{-1}, 0.75 gL^{-1},1 gL^{-1}, 1.5 gL$^{-1}$ catalyst doses was observed to be 60.56%, 74.89%, 81.56%, 80.37%, 75.68% and 68.31% respectively. The photocatalytic efficiency first increases with the increase in catalyst dose but with further increase it decreases. The increase in photocatalytic efficiency from increasing catalyst dose from 0.1 gL^{-1} to 0.5 gL^{-1} confirms the increase in active sites for the pollutant on the surface of catalyst. But decline after further increase in catalyst dose is due to the fact that due to agglomeration of catalyst powder and also more active sites will be available for less pollutant are the main reasons for decline in degradation from increasing the catalyst amount from 0.5 gL^{-1} to 1.5 gL^{-1}(Yan et al., 2015).
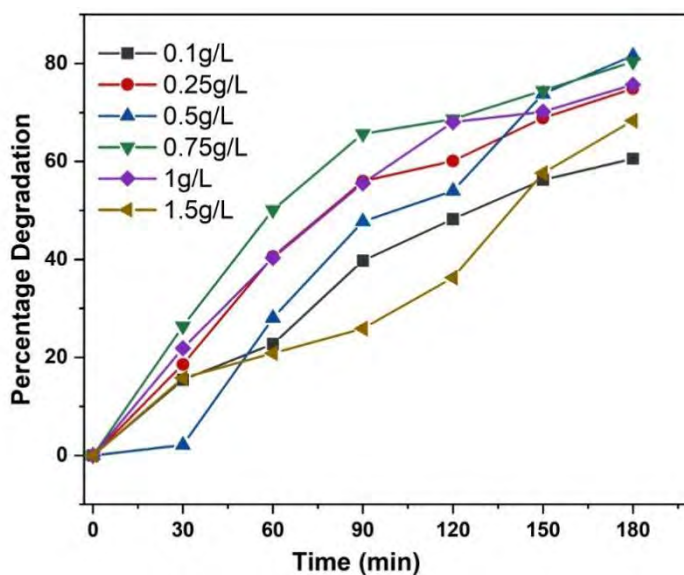
Figure 3.8: Effect of catalyst (1% Al-ZnTiO$_3$) dose on 2-Chlorophenol degradation efficiency under solar radiation (2-Chlorophenol concentration = 100 mgL^{-1}, irradiation time = 180 minutes)

3.6. Initial Concentration of Pollutant

Initial concentration is very important for better understanding of photocatalytic degradation of the pollutant. Degradation of 2-CP was analyzed by varying the initial concentrations (20 mgL^{-1}, 50 mgL^{-1}, 75 mgL^{-1}, 100 mgL^{-1}). The highest degradation level of about 98.98% was achieved at 20 mgL^{-1} following 96.01% degradation at 50 mgL^{-1}, 90.20% degradation at 75 mgL^{-1} and 81.60% degradation at 100 mgL^{-1} as shown in figure 3.9.
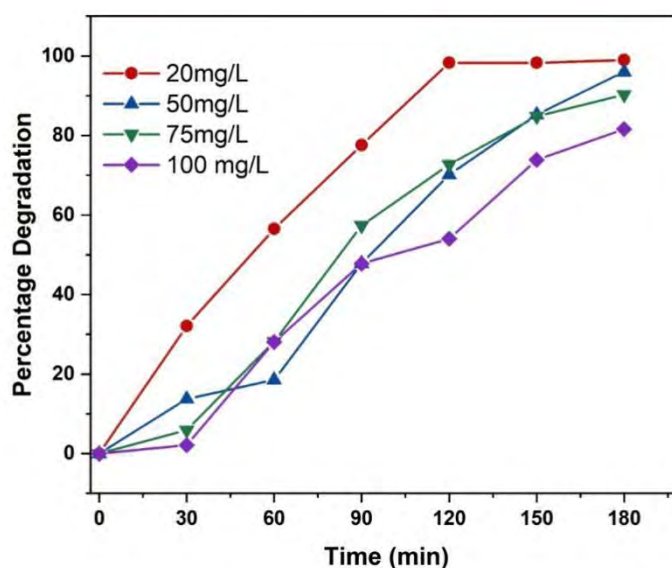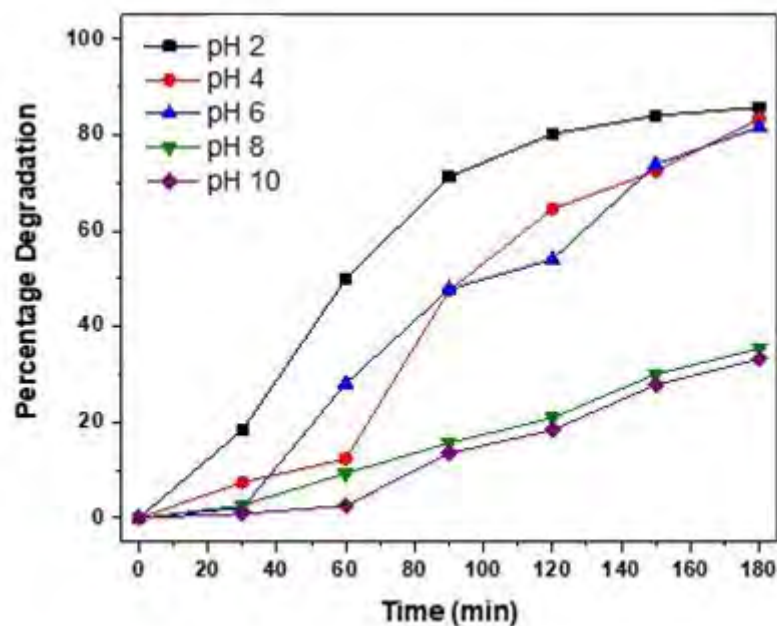

Figure 3.9: Effect of initial concentration of the 2-Chlorophenol, on degradation efficiency under solar radiation (Catalyst dose = 0.5gL^{-1}, pH = 6, irradiation time = 180 minutes)

There is decrease in photocatalytic activity by increasing. This can be attributed to the decreased likelihood of 2-CP molecules to react with the active species on the surface of 1% Al-ZnTiO$_3$ with increase in initial concentration (Rashid & Barakat, 2014).

3.7. Effect of pH

Solution pH affects the surface charge of the photocatalyst hence it accounts for significant influence on photocatalysis. Experiments were conducted with different solution pH (2, 4, 8 & 10) to check that which one will give the best results. Effect of different pH on photocatalysis is shown in Figure 3.10. Degradation of 2CP was increased with the decrease in pH. The percentage degradation at pH 2, pH 4, pH 6, pH 8, pH 10 were 85.73%, 83.30%, 81.60%, 35.36% and 33.24% respectively keeping the same conditions (Catalyst dose = 0.5gL^{-1}, 2-Chlorophenol concentration = 100 mgL^{-1}, irradiation time = 180 minutes). The increase in degradation efficiency is observed with the decreasing pH and the maximum degradation was observed at pH 2. Acidic pH shows good degradation efficiency and the basic pH hindered degradation efficiency of the catalyst (Yan et al., 2015). Generally, the influence of pH on the photocatalytic degradation refer to the absorption on the surface of the photocatalyst and its relationship with the ionic form (anion or cation) of the organic pollutant. Electrostatic attraction or repulsion between organic molecule and the catalytic surface takes place, and the photocatalytic degradation rate is consequently inhibited or enhanced, respectively. The point of zero catalyst of a catalyst is calculated by salt (KCl) addition method was turn out to be 6.19. At pH above 6.19, zinc titanate surface bears negative charge and electrostatic repulsion between aqueous phenolate ions and ZnTiO$_3$ may be responsible for lower adsorption and corresponding degradation efficiency. Higher pH have also been reported to decrease the degradation rates due to OH$^-$ ions scavenging by thus formed carbonate ions. (Rashid & Barakat, 2014).

Figure 3.10: Influence of initial concentration of the 2-Chlorophenol, on degradation efficiency under solar radiation (Catalyst dose = 0.5gL^{-1}, pH = 6, irradiation time = 180 minutes)
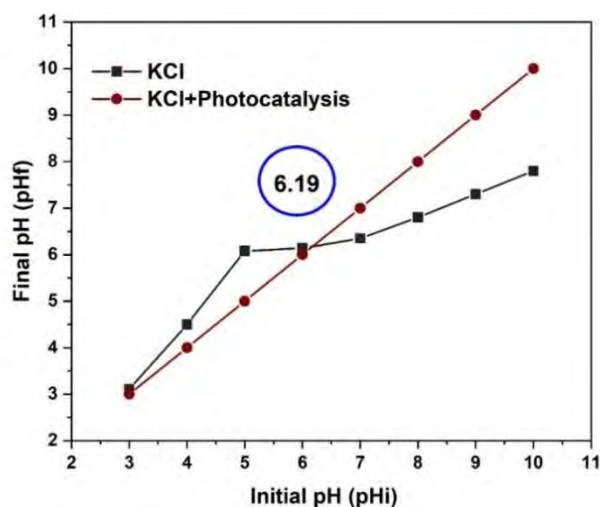
Figure 3.11: Point of zero charge of 1% Al-ZnTiO$_3$

3.8. Reusability experiments:

The reusability and stability of the photocatalyst, besides the photocatalysis, are very important factors when the catalyst has to be used at a large scale. In order to investigate the efficiency and stability of a photocatalyst additional runs of 2-CP were conducted by reusing the photocatalyst. Four successive experiments of the reused catalyst were conducted as shown in Figure 3.12. For the reusability test the spent photocatalyst washed several times

with deionized water, then centrifuged and was dried at 80°C before the next cycle (Alafif et al., 2019). It could be seen in the results that the degradation efficiency decreased from in 4 cycles from 81.56% to 74.86%, 66.98% and 59.12% for the respective reused catalyst. The decline in photocatalytic activity of photocatalyst refer to the accumulation of intermediates on the surface of photocatalyst and portable loss of during the recollection (Harifi & Montazer, 2014). The result also indicates high efficiency of the catalyst as it shows around 8% decrease in the degradation activity after every use. The results also clearly showed that 1% Al-ZnTiO$_3$ is highly stable photocatalyst and could be reused numerous times (Teixeira et al., 2016).
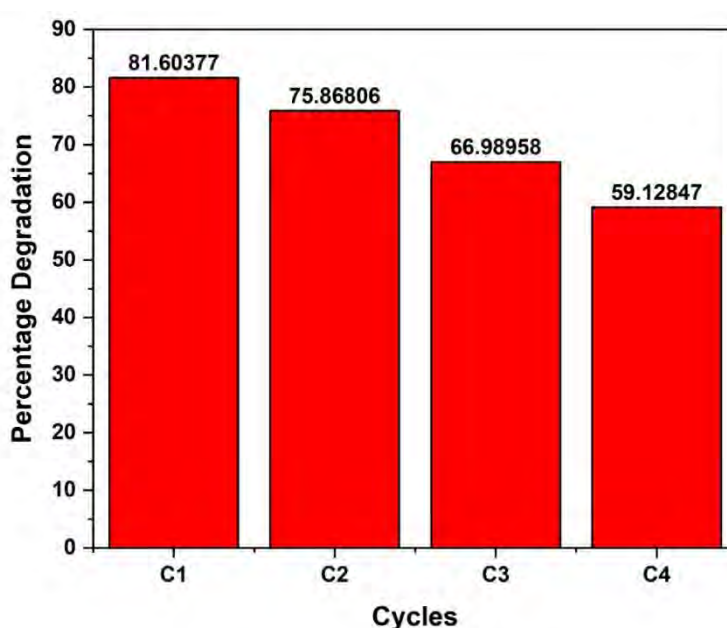
Figure 3.12: Effect of reused 1% Al-ZnTiO$_3$ on 2CP degradation (Catalyst dose = 0.5gL^{-1}, pH = 6, irradiation time = 180 minutes, Initial Concentration of 2CP = 100mgL^{-1})

3.9. Activity test:

To investigate the bit part of the important reactive components in the photocatalytic degradation of 2-Chlorophenol a chain of experiments was conducted by adding some scavenger chemicals (benzoquinone, Na$_2$SO$_4$, EDTA, isopropyl alcohol). The benzoquinone, Na$_2$SO$_4$, Ethylene-diamine-tetra acetic acid and isopropyl alcohol were used for scavenging superoxide ions, electrons, holes and hydroxyl radicals respectively. All the scavengers played role in the degradation. The results showed that using BQ and Na$_2$SO$_4$ significant decline in photocatalytic degradation of 2CP. While using IPA and EDTA the degradation doesn't show significant effect on photo-catalysis. It revealed that O$_2^-$ and e$^-$ played a major role in the 2-Chlorophenol degradation over 1% Al-ZnTiO$_3$.
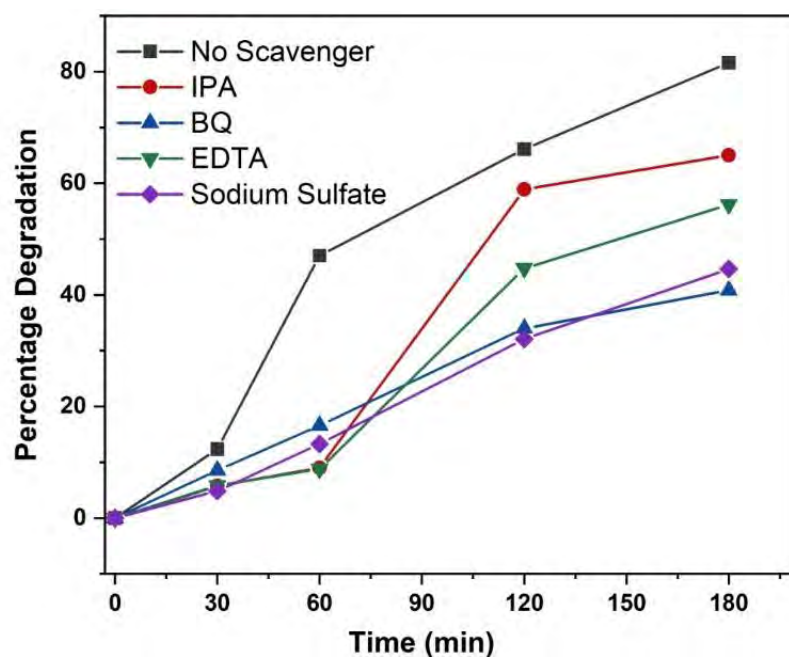
Figure 3.13: Degradation efficiency of 1% Al-ZnTiO$_3$ by using different scavengers on 2-CP (2-CP Concentration = 100mgL^{-1}, Catalyst Dose=0.5gL^{-1})

3.10.   Reaction kinetics:

The photocatalysis mostly follows a Langmuir Hinshelwood mechanism (Yan et al., 2015). The rate of photocatalysis of 2-CP was evaluated with the help of first order, second order and zero order (Von Moos et al., 2012). The equations used for this purpose are given below:

$\ln (C_o/C_t) = kt$ eq 3.3

$1/C_o=1/C_t+kt$ eq 3.4

$C_o-C_t= kt$ eq 3.5

Where C_o is the initial concentration of 2-CP, C_t is the concentration of 2-CP at any time (t), k is the rate constant (min^{-1}) in the above equations. Kinetic studies graphs were plotted between $\ln(C_o/C_t)$, $1/C_t$, Co-Ct on y-axis against time (t) on x-axis for all parameters like catalyst dose, pH effect and pollutant concentration. The regression coefficient (R^2) and the visible rate constant (k) values taken from the regression plots are given in the Table 3.1. The results revealed that first order kinetics perfectly explains the rate of degradation of 2-CP. The increase in concentration of 2-CP has decreased the degradation rate from 0.02318 to 0.01081 per minute. From the pH, the highest rate was observed at pH 2 that means acidic conditions will favor the degradation of 2-CP. The most suitable catalyst dose came out to be 0.5g/L which shows highest rate 0.49304 among all catalyst doses.

Table 3.1: Reaction Kinetic values that are explaining the effect of pH and 2-CP concentration & catalyst dose, over 1% Al-ZnTiO$_3$

Experiment	Conditions	First order		Second order		Zero order	
		k (min^{-1})	R^2	k (min^{-1})	R^2	k (min^{-1})	R^2
Effect of Catalyst dose (gL^{-1})	0.1	0.00490	0.97661	0.00731	0.96310	0.00350	0.97359
	0.25	0.08780	0.96947	0.01590	0.83400	0.00452	0.89555
	0.5	0.01080	0.98461	0.02760	0.84300	0.00416	0.97525
	0.75	0.00800	0.88672	0.01893	0.95220	0.00484	0.91758
	1	0.01025	0.90214	0.02411	0.80755	0.00534	0.94539
	1.5	0.00600	0.90214	0.00943	0.81668	0.00417	0.95922
Effect of 2-CP concentration (mgL^{-1})	100	0.01081	0.98153	0.02760	0.84381	0.00416	0.97525
	75	0.01381	0.95840	0.07222	0.82890	0.00382	0.96240
	50	0.01691	0.84391	0.20316	0.56974	0.00288	0.97585
	20	0.02891	0.89746	1.88091	0.81821	0.00163	0.89024
Effect of pH	2	0.01316	0.94882	0.04724	0.98091	0.00519	0.80243
	4	0.01073	0.95718	0.02577	0.85372	0.00565	0.96455
	6	0.01081	0.98153	0.02875	0.72875	0.00527	0.93956
	8	0.00292	0.77146	0.00325	0.80547	0.00265	0.83150
	10	0.00285	0.69570	0.00310	0.74434	0.00265	0.7438
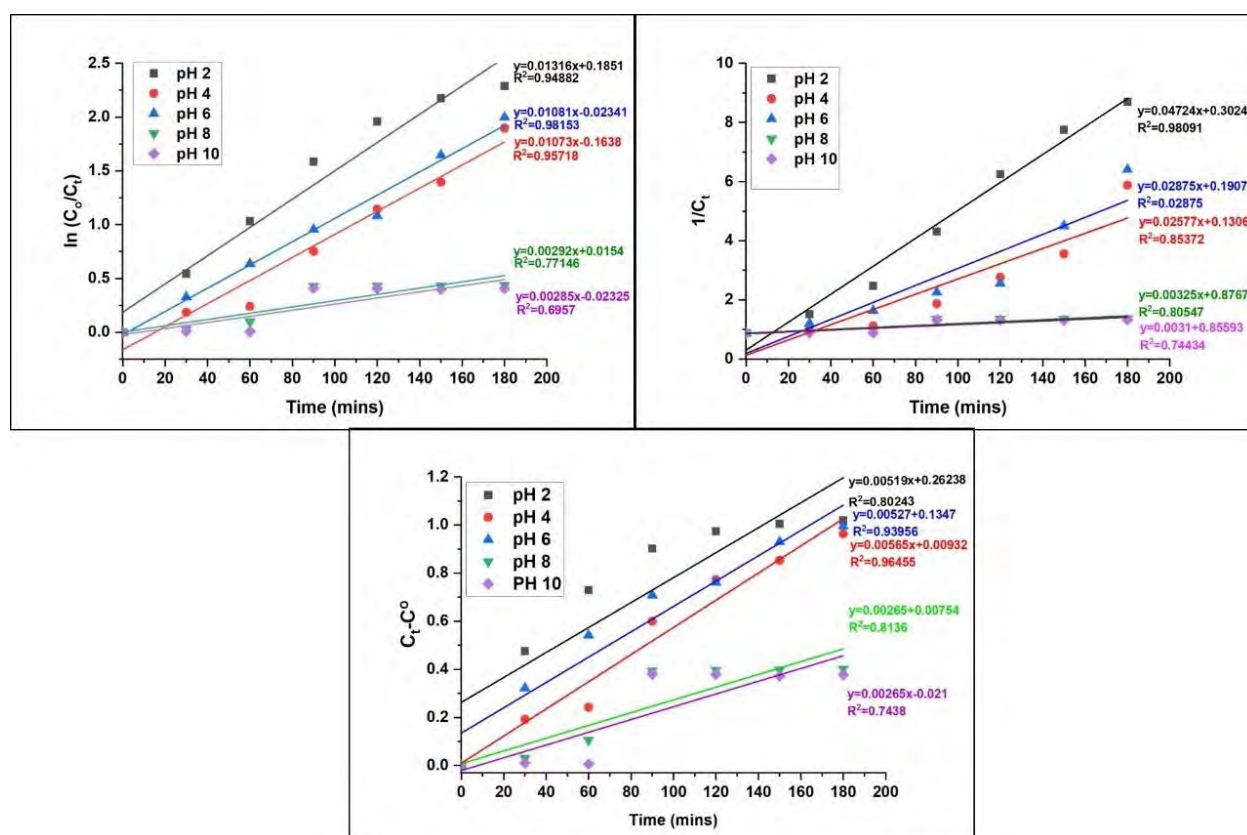
Figure 3.14: The **(a)** First order **(b)** second order and **(c)** zero order kinetic model of 2-Chlorophenol degradation at different pH
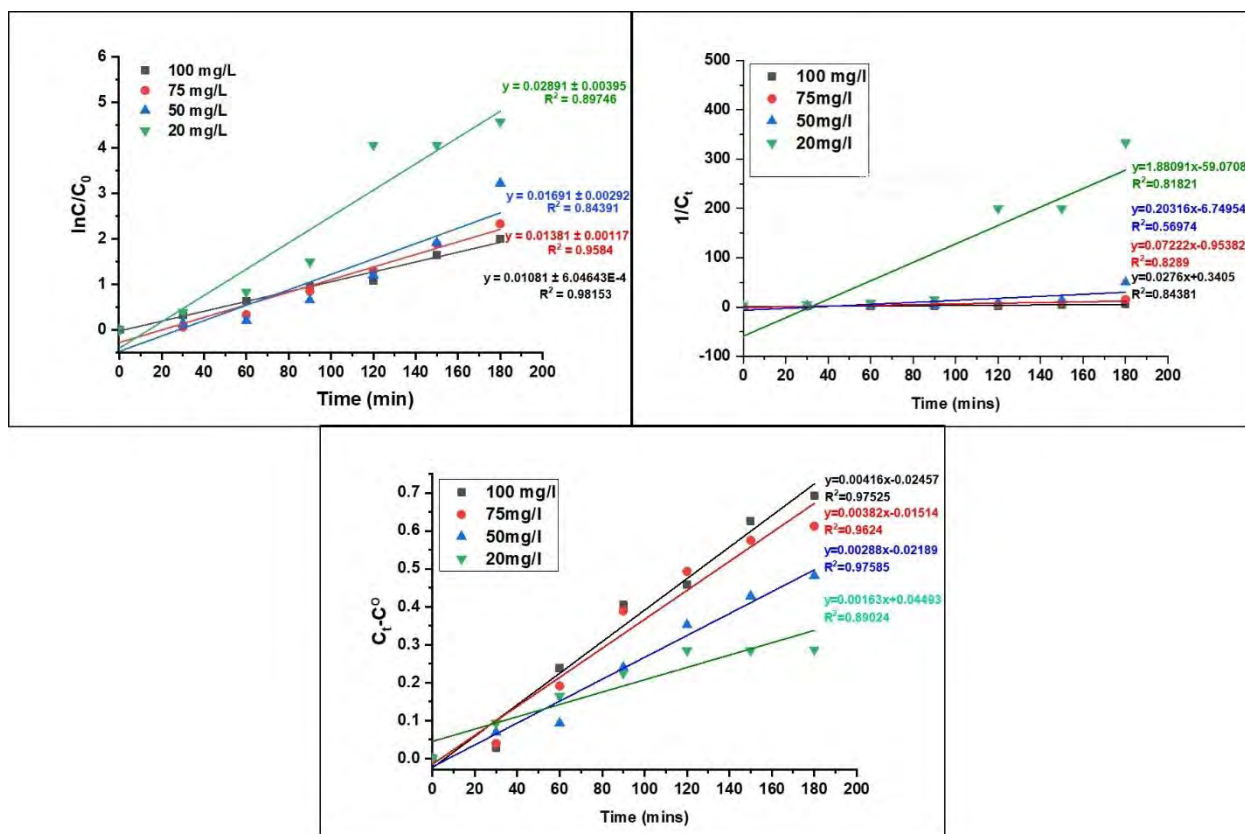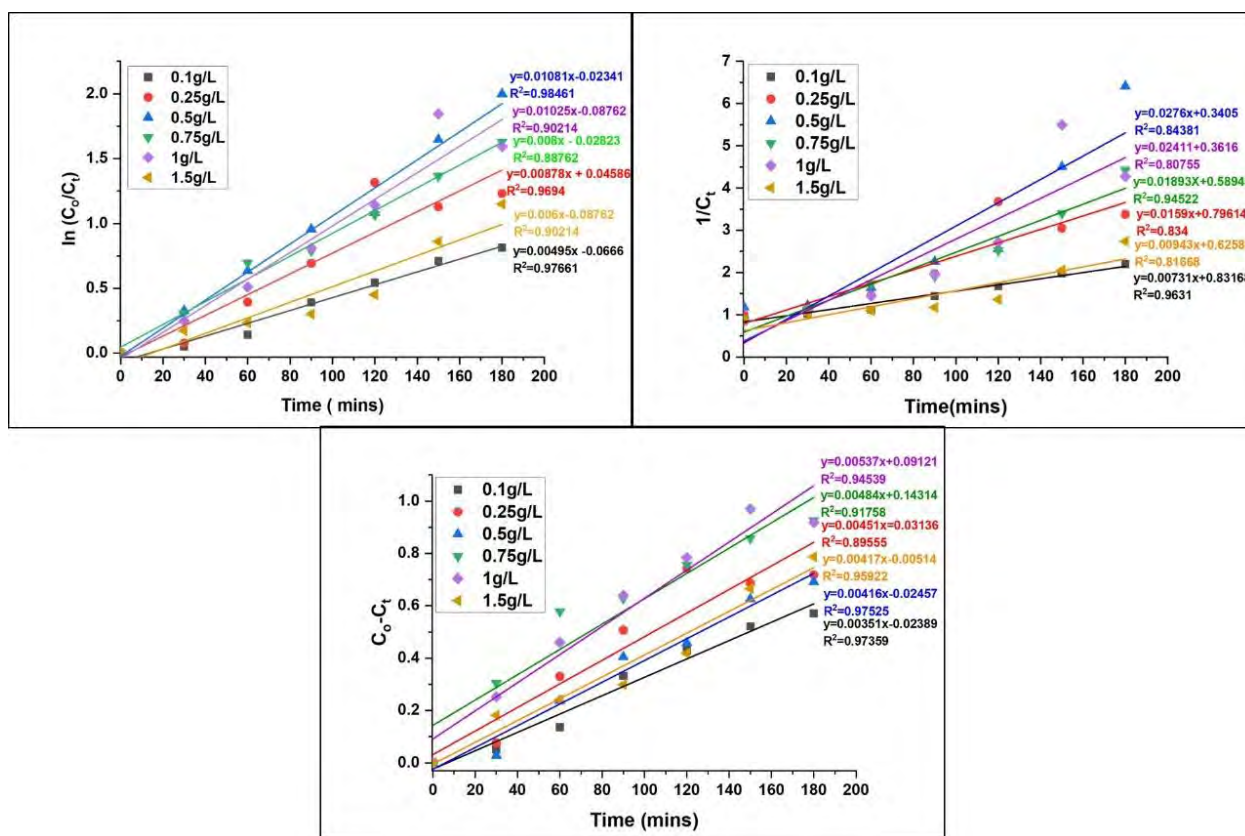
Figure 3.15: The **(a)** First order **(b)** second order and **(c)** zero order kinetic model of 2-Chlorophenol degradation at different concentrations

Figure 3.16: The **(a)** First order **(b)** second order and **(c)** zero order kinetic model of 2-Chlorophenol degradation at different catalyst dose

3.11.   UV-Visible Absorption Spectra

The absorbance spectrum shows absorption at each wavelength of the 2CP in the presence different catalysts. **Fig. 3.17** shows the UV-Visible absorption spectra of 2CP and its photocatalytic degradation within 180 minutes. All the experiments were done at same conditions (Catalyst dose = $0.5gL^{-1}$, 2-Chlorophenol concentration = 100 mgL^{-1}) under direct sunlight. There is significant increase observed with the passage of time for all catalysts. But the highest percentage degradation was observed for 1% $Al-ZnTiO_3$ i.e. 81.60 followed by 3% $Al-ZnTiO_3$, Pure $ZnTiO_3$, TiO_2 nanotubes with the percentage degradation of 76.37, 70.34 and 52.79 respectively.
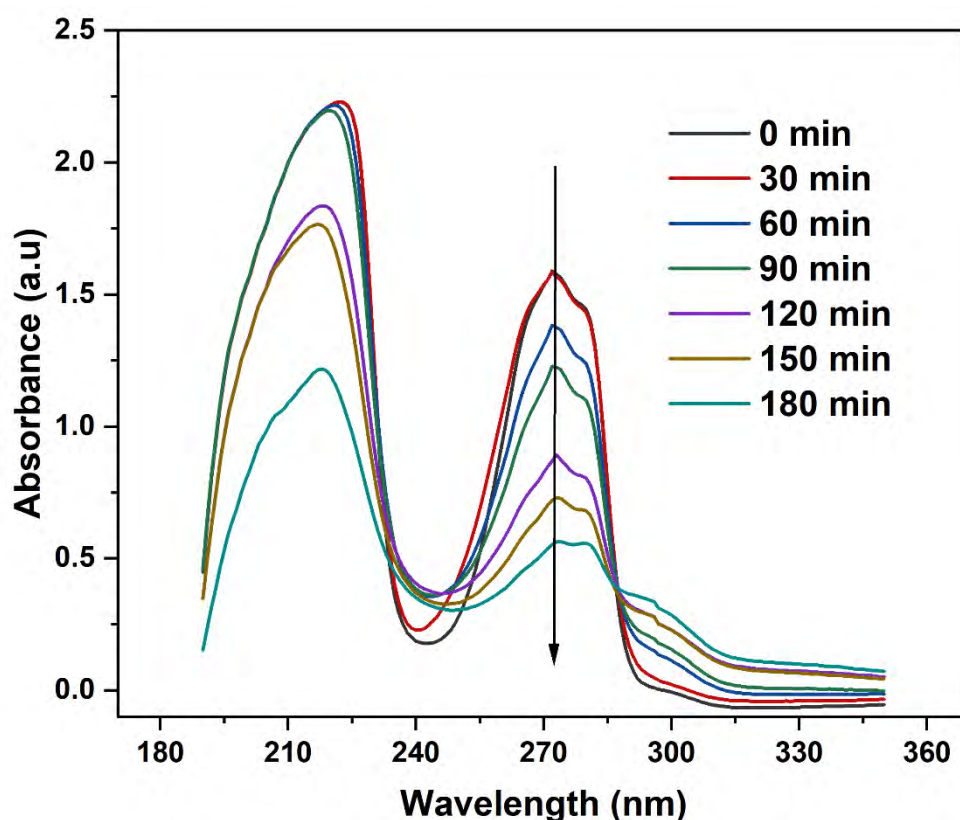
Figure 3.17: UV-visible spectrum of 2CP degradation over $Al-ZnTiO_3$ (2CP concentration = 100mgL^{-1}, catalyst dose = $0.5gL^{-1}$, pH = 6)

3.12.   Degradation mechanism of 2-CP over 1% $Al-ZnTiO_3$

Zinc titanate has large comparatively wider energy band gap (~3eV) and Aluminum doping was done to minimize the band gap and provide electrons a fermi layer to stay and perform degradation effectively. When solar light falls on photo-catalyst it results in the excitation of

$ZnTiO_3$ to produce electron and holes. The electrons produced by solar light in the conduction band of Al-$ZnTiO_3$ can produce superoxide radical by the absorbed O_2 due to its more negative valance edge (Surendar et al., 2014). Whereas the holes on the valance band oxidized H_2O, to yield hydroxyl radical because of the more positive conduction edges. Finally, the degradation of 2-CP was performed mostly superoxide ions and electrons (above 60%) and hydroxide ions (below 40%).
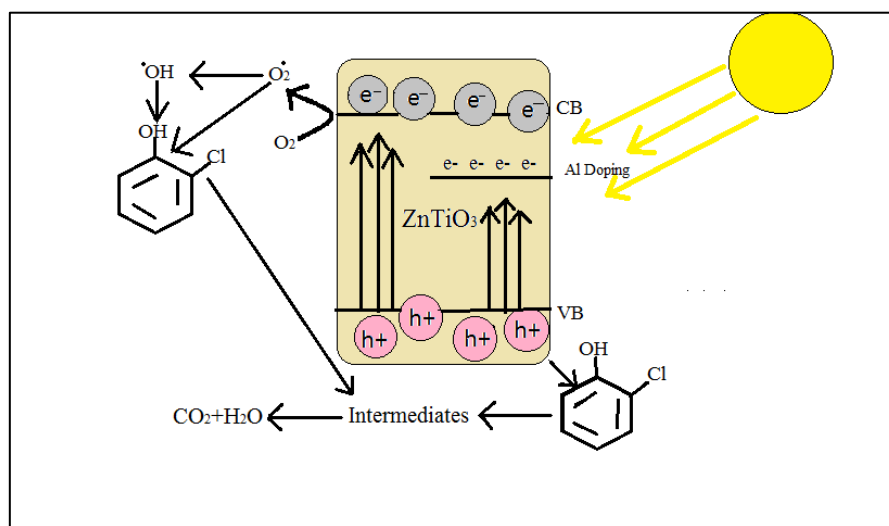
Figure 3.18: Proposed Catalytic Degradation Mechanism of 2-Chlorophenol over 1% Al-$ZnTiO_3$ under direct sunlight

4. CONCLUSION

The simple one, two and three steps synthesis route has been developed for the preparation of titania nanotubes, $ZnTiO_3$ and Aluminum (1% and 3%) doped $ZnTiO_3$ nanoparticles, respectively. The XRD studies confirmed the crystallinity of the as per synthesized particles. The PL results showed significant reduction in the recombination rate of the photo-induced electron and hole pairs in 1% Aluminum doped $ZnTiO_3$ nanoparticles. UV visible spectrophotometry results confirmed high photocatalytic activity of synthesized nanocomposite in direct solar light. Photocatalytic degradation test showed maximum (81.6%) degradation of 2-Chlorophenol by 1% Al-$ZnTiO_3$. All four catalysts i.e., titania nanotubes, $ZnTiO_3$, Aluminum (1% and 3%) doped $ZnTiO_3$, used during the study have shown minimal adsorption and photolysis that confirmed the catalyst is significantly solar light active. All the catalyst has shown optimum results at 100 mgL^{-1}, 2-Chlorophenol concentration, $0.5gL^{-1}$ catalyst dose and pH 6. Reusability tests clearly showed that 1% Al-$ZnTiO_3$ is highly stable photocatalyst and could be reused numerous times. This study hence confirmed that 1% Aluminum doped $ZnTiO_3$ is effective for the degradation of 2-Chlorophenol under direct sunlight.

5. REFERENCES

Abirami, R., Senthil, T. S., Keerthana, S. P., Yuvakkumar, R., Ravi, G., Pannipara, M., & Al-sehemi, A. G. (2021). *An approach to enhance the photocatalytic activity of ZnTiO 3*. *47*(December 2020), 18122–18131.

Ajmal, A., Majeed, I., Malik, R. N., Idriss, H., & Nadeem, M. A. (2014). Principles and mechanisms of photocatalytic dye degradation on TiO 2 based photocatalysts: A comparative overview. *RSC Advances*, *4*(70), 37003–37026.

Alafif, Z. O., Anjum, M., Kumar, R., Abdelbasir, S. M., & Barakat, M. A. (2019). Synthesis of CuO–GO/TiO2 visible light photocatalyst for 2-chlorophenol degradation, pretreatme nt of dairy wastewater and aerobic digestion. *Applied Nanoscience (Switzerland)*, *9*(4), 579–591.

Alshabib, M., & Onaizi, S. A. (2019). A Review on Phenolic Wastewater Remediation using Homogeneous and Heterogeneous Enzymatic Processes: Current Status and Potential Challenges. *Separation and Purification Technology*, *219*, 186–207.

Barakat, M. A., Kumar, R., Rashid, J., Seliem, M. K., Al-Mur, B., & El-Shishtawy, R. M. (2020). A novel CuO–Cu2O/Ag–Ag3PO4 nanocomposite: Synthesis, characterization, and its application for 2-chlorophenol decontamination under visible light. *Journal of the Taiwan Institute of Chemical Engineers*, *115*, 208–217.

Campaña, A. L., Florez, S. L., Noguera, M. J., Fuentes, O. P., Puentes, P. R., Cruz, J. C., & Osma, J. F. (2019). Enzyme-Based Electrochemical Biosensors for Microfluidic Platforms to Detect Pharmaceutical Residues in Wastewater. *Biosensors*, *9*(1), 41.

Chakrabarti, S., & Dutta, B. K. (2004). Photocatalytic degradation of model textile dyes in wastewater using ZnO as semiconductor catalyst. *Journal of Hazardous Materials*, *112*(3), 269–278.

Chang, Y.-S., Chang, Y.-H., Chen, I.-G., Chen, G., & Chai, Y.-L. (2002). Synthesis and Characterization of Zinc Titanate Nano-Crystal Powders by Sol-Gel Technique. *Journal of Crystal Growth*, *243*, 319–326.

Chen, F., Yu, C., Wei, L., Fan, Q., Ma, F., Zeng, J., Yi, J., Yang, K., & Ji, H. (2020). Science of the Total Environment Fabrication and characterization of ZnTiO 3 / Zn 2 Ti 3 O 8 / ZnO ternary photocatalyst for synergetic removal of aqueous organic pollutants and Cr (

VI) ions. *Science of the Total Environment*, *706*, 136026.

Cheruvu, H. S., Liu, X., Grice, J. E., & Roberts, M. S. (2020). Modeling percutaneous absorption for successful drug discovery and development. *Expert Opinion on Drug Discovery*, *15*(10), 1181–1198.

Conesa, J. C. (2013). Band structures and nitrogen doping effects in zinc titanate photocatalysts. *Catalysis Today*, *208*, 11–18.

Delgado, F., Gutierrez, V. S., Dennehy, M., & Alvarez, M. (2020). Stable and efficient metal-biochar supported catalyst: degradation of model pollutants through sulfate radical-based advanced oxidation processes. *Biochar*, *2*(3), 319–328.

Gao, Z., & Qu, X. (2020). Construction of ZnTiO3/Bi4NbO8Cl heterojunction with enhanced photocatalytic performance. *Nanoscale Research Letters*, *15*(1).

Gholami, A., Amirabad, T. N., & Maddahfar, M. (2017). Investigation of photovoltaic properties of silver-doped ZnTiO3 nanoparticles. *Journal of Materials Science: Materials in Electronics*, *28*(20), 15327–15332.

Gonzales, L. L., da Silva Hartwig, M., Fassbender, R. U., Moreira, E. C., Pereira, M. B., Jardim, P. L. G., Raubach, C. W., Moreira, M. L., & da Silva Cava, S. (2021). Properties of zinc titanates synthesized by microwave assisted hydrothermal method. *Heliyon*, *7*(3).

Gubin, A., Sukhanov, P., Kushnir, A., Shikhaliev, K., Potapov, M., & Kovaleva, E. (n.d.). Monitoring of phenols in natural waters and bottom sediments: preconcentration on a magnetic sorbent, GC–MS analysis, and weather observations. *Chemical Papers*, *75*(4), 1445–1456.

Gül, Ş., & Özcan-Yildirim, Ö. (2009). Degradation of Reactive Red 194 and Reactive Yellow 145 azo dyes by O3 and H2O2/UV-C processes. *Chemical Engineering Journal*, *155*(3), 684–690.

Harifi, T., & Montazer, M. (2014). A novel magnetic reusable nanocomposite with enhanced photocatalytic activities for dye degradation. *Separation and Purification Technology*, *134*, 210–219.

Hashimoto, K., Irie, H., & Fujishima, A. (2005). TiO 2 photocatalysis: A historical overview and future prospects. *Japanese Journal of Applied Physics, Part 1: Regular Papers and Short Notes and Review Papers*, *44*(12), 8269–8285.

Jaramillo-Fierro, X., González, S., Jaramillo, H. A., & Medina, F. (2020). Synthesis of the zntio3 /tio2 nanocomposite supported in ecuadorian clays for the adsorption and photocatalytic removal of methylene blue dye. *Nanomaterials*, *10*(9), 1–20.

Kaushik, R., Samal, P. K., & Halder, A. (n.d.). *Supporting Information Degradation of Fluoroquinolone-Based Pollutants and Bacterial Inactivation by Visible-Light-Active Al-Doped*. 1–12.

Kumar, A. (2017). A Review on the Factors Affecting the Photocatalytic Degradation of Hazardous Materials. *Material Science & Engineering International Journal*, *1*(3).

Madhavan, J., Maruthamuthu, P., Murugesan, S., & Anandan, S. (2008). Kinetic studies on visible light-assisted degradation of acid red 88 in presence of metal-ion coupled oxone reagent. *Applied Catalysis B: Environmental*, *83*(1–2), 8–14.

Melati, I., Maghfiroh, M., & Jasalesmana, T. (2020). Public perception and contribution of domestic waste to water pollution of Lake Matano, South Sulawesi-Indonesia. *IOP Conference Series Earth and Environmental Science*, *535*(1), 12065.

Mulla, S. I., Bharagava, R. N., Belhaj, D., Saratale, G. D., Kumar, A., Rajasekar, A., Tallur, P. N., Edalli, V. A., Hu, A., & Yu, C.-P. (2019). Microbial Degradation of Phenolic Compounds. In *Microbes and Enzymes in Soil Health and Bioremediation* (pp. 305–320).

Multari, S., Carlin, S., Sicari, V., & Martens, S. (2020). Differences in the composition of phenolic compounds, carotenoids, and volatiles between juice and pomace of four citrus fruits from Southern Italy. *European Food Research and Technology*, *246*(10), 1991–2005.

Naik, S., & Eswari, J. S. (2021). Experimental and validation with neural network time series model of microbial fuel cell bio-sensor for phenol detection. *Journal of Environmental Management*, *290*, 112594.

Nakata, K., & Fujishima, A. (2012). TiO$_2$ photocatalysis: Design and applications. *Journal of Photochemistry and Photobiology C: Photochemistry Reviews*, *13*(3), 169–189.

Ndebele, N., Mgidlana, S., & Nyokong, T. (n.d.). Electrocatalytic Activity of Cobalt Phthalocyanines Revisited: Effect of the Number of Oxygen Atoms and Conjugation to Carbon Nanomaterials. *Electrocatalysis*, 1–17.

Nthunya, L. N., Khumalo, N. P., Verliefde, A. R., Mamba, B. B., & Mhlanga, S. D. (2019). Quantitative analysis of phenols and PAHs in the Nandoni Dam in Limpopo Province, South Africa: A preliminary study for dam water quality management. *Physics and Chemistry of the Earth Parts A/B/C*, *112*, 228–236.

Online, V. A., Surendar, T., Kumar, S., & Shanker, V. (2014). *Influence of La-doping on phase transformation*. 728–735.

Pandey, D., Singh, S., Dutta, K., Daverey, A., & Arunachalam, K. (2021). Biochar-Based Nanocomposites: A Sustainable Solution for Water and Wastewater Treatment. In *Biobased Nanotechnology for Green Applications* (pp. 619–639).

Perween, S., & Ranjan, A. (2017). Solar Energy Materials & Solar Cells Improved visible-light photocatalytic activity in ZnTiO 3 nanopowder prepared by sol-electrospinning. *Solar Energy Materials and Solar Cells*, *163*(January), 148–156.

Pirgholi-Givi, G., Azizian-Kalandaragh, Y., & Farazin, J. (2021). Comparison of the photocatalytic activity of perovskite structures: Bismuth, barium, and zinc titanate nanostructures for photodegradation of methylene blue from water. *Journal of Photochemistry and Photobiology A: Chemistry*, *408*(September 2020), 113104.

Rahemi, V., Trashin, S., Hafideddine, Z., Meynen, V., Van Doorslaer, S., & De Wael, K. (2019). Enzymatic sensor for phenols based on titanium dioxide generating surface confined ROS after treatment with H2O2. *Sensors and Actuators B Chemical*, *283*, 343–348.

Rashid, J., & Barakat, M. A. (2014). *Ag 3 PO 4 Enhanced TiO 2 for Visible Light Photocatalysis of 2-Chlorophenol in Wastewater*. 3–7.

Rashid, J., Barakat, M. A., Ruzmanova, Y., & Chianese, A. (2015). Fe3O4/SiO2/TiO2 nanoparticles for photocatalytic degradation of 2-chlorophenol in simulated wastewater. *Environmental Science and Pollution Research*, *22*(4), 3149–3157.

Sosnin, I. M., Vlassov, S., Akimov, E. G., Agenkov, V. I., & Dorogin, L. M. (n.d.). Transparent ZnO-coated polydimethylsiloxane-based material for photocatalytic purification applications. *Journal of Coatings Technology and Research*, *17*(2), 573–579.

Surendar, T., Kumar, S., & Shanker, V. (2014). Influence of La-doping on phase

transformation and photocatalytic properties of ZnTiO3 nanoparticles synthesized via modified sol-gel method. *Physical Chemistry Chemical Physics*, *16*(2), 728–735.

Teixeira, S., Martins, P. M., Lanceros-Méndez, S., Kühn, K., & Cuniberti, G. (2016). Reusability of photocatalytic TiO 2 and ZnO nanoparticles immobilized in poly(vinylidene difluoride)-co-trifluoroethylene. *Applied Surface Science*, *384*, 497–504.

Von Moos, N., Burkhardt-Holm, P., & Köhler, A. (2012). Uptake and effects of microplastics on cells and tissue of the blue mussel Mytilus edulis L. after an experimental exposure. *Environmental Science and Technology*, *46*(20), 11327–11335.

Wang, C., Xu, Y. J., Shi, Y., Wang, C., Duan, L., Gu, W., Ruan, H. J., Zhang, S. P., Zhi, H., Kong, J., Zhang, L. X., Zhang, M., & Zhang, H. W. (2020). Verification on the Developmental Toxicity of Short-term Exposure to Phenol in Rats. *Biomedical and Environmental Sciences*, *33*(6), 403–413.

Wang, H., Fu, Y., Han, T., Wan, J., & Zheng, X. (2015). Adsorption and photocatalytic behavior of titanate nanotubes sensitized with zinc tetra(4-carboxyphenyl) porphyrin. *RSC Advances*, *5*(42), 33570–33578.

Wang, Y. W., Yuan, P. H., Fan, C. M., Wang, Y., Ding, G. Y., & Wang, Y. F. (2012). Preparation of zinc titanate nanoparticles and their photocatalytic behaviors in the photodegradation of humic acid in water. *Ceramics International*, *38*(5), 4173–4180.

Wu, Y., Zhang, N., & de Lannoy, C.-F. (2021). Upcycling wildfire-impacted boreal peats into porous carbons that efficiently remove phenolic micropollutants. *Journal of Environmental Chemical Engineering*, *9*(4), 105305.

Yan, X., Zhao, C. L., Zhou, Y. L., Wu, Z. J., Yuan, J. M., & Li, W. S. (2015). Synthesis and characterization of ZnTiO3 with high photocatalytic activity. *Transactions of Nonferrous Metals Society of China (English Edition)*, *25*(7), 2272–2278.

Zango, Z. U., Sambudi, N. S., Jumbri, K., Ramli, A., Abu Bakar, N. H. H., Saad, B., Rozaini, M. N. H., Isiyaka, H. A., Osman, A. M., & Sulieman, A. (2020). An Overview and Evaluation of Highly Porous Adsorbent Materials for Polycyclic Aromatic Hydrocarbons and Phenols Removal from Wastewater. *Water*, *12*(10), 2921.

Zhao, J., Otgonbayar, Z., Fatema, K. N., Sagadevan, S., & Oh, W.-C. (2020). Novel-

structured mesoporous SiO2 and ZrO2–GO nanocomposite for photocatalytic degradation of toxic phenolic derivatives under the visible light irradiation. *Surfaces and Interfaces*, *20*, 100613.

Zhao, Z., An, H., Lin, J., Feng, M., Murugadoss, V., Ding, T., Liu, H., Shao, Q., Mai, X., Wang, N., Gu, H., Angaiah, S., & Guo, Z. (2019). Progress on the Photocatalytic Reduction Removal of Chromium Contamination. *Chemical Record*, *19*(5), 873–882.

Shang, N. C., Yu, Y. H., Ma, H. W., Chang, C. H., & Liou, M. L. (2006). Toxicity measurements in aqueous solution during ozonation of mono-chlorophenols. Journal of environmental management, 78(3), 216-222

Sharma, S., Sinha, A. K., & Singh, A. P. (2019). Synthesis and Characterization of $ZnTiO_3$ Nanoparticles by Sol-Gel Method. Journal of Nanotechnology, 2019.

Sas, O. G., Castro, M., Domínguez, Á., & González, B. (2019). Removing phenolic pollutants using deep eutectic solvents. Separation and Purification Technology, 227, 115703

Khezami, L., & Capart, R. (2005). Adsorption of $ZnTiO_3$ nanocrystallites at the water–silica interface. Journal of colloid and interface science, 284(1), 105-112